

LEVEL

(12)
B3

AD A101540



LOW-SPEED AERODYNAMIC CHARACTERISTICS OF A SMALL, FIXED-TRAILING-EDGE CIRCULATION CONTROL WING CONFIGURATION FITTED TO A SUPERCRITICAL AIRFOIL

by

Robert J. Englar

**APPROVED FOR PUBLIC RELEASE:
DISTRIBUTION UNLIMITED**

AVIATION AND SURFACE EFFECTS DEPARTMENT

DTNSRDC/ASED-81/08

March 1981

**DAVID
W.
TAYLOR
NAVAL
SHIP
RESEARCH
AND
DEVELOPMENT
CENTER**

**BETHESDA
MARYLAND
20084**

**DTIC
ELECTE
JUL 20 1981**

**A
81 7**

DTIC FILE COPY

92
X

UNCLASSIFIED

(16) F414-1

SECURITY CLASSIFICATION OF THIS PAGE (When Data Entered)

14 REPORT DOCUMENTATION PAGE		READ INSTRUCTIONS BEFORE COMPLETING FORM	
1. REPORT NUMBER DTNSRDC/ASED-81/08	2. GOVT ACCESSION NO. AD A101540	3. RECIPIENT'S CATALOG NUMBER 9	
4. TITLE (and Subtitle) LOW-SPEED AERODYNAMIC CHARACTERISTICS OF A SMALL, FIXED-TRAILING-EDGE CIRCULATION CONTROL WING CONFIGURATION FITTED TO A SUPERCRITICAL AIRFOIL		5. TYPE OF REPORT & PERIOD COVERED Final Report, Mar 1980 - Jan 1981	
7. AUTHOR(s) Robert J. Englar		8. CONTRACT OR GRANT NUMBER(s)	
9. PERFORMING ORGANIZATION NAME AND ADDRESS David Taylor Naval Ship R&D Center Aviation and Surface Effects Department Bethesda, Maryland 20084		10. PROGRAM ELEMENT, PROJECT, TASK AREA & WORK UNIT NUMBERS ZF 41421001 (1660-608) WF 41421000 (1600-081)	
11. CONTROLLING OFFICE NAME AND ADDRESS Naval Air Systems Command AIR-320D Washington, D.C. 20361		12. REPORT DATE March 1981	
14. MONITORING AGENCY NAME & ADDRESS (if different from Controlling Office) Naval Material Command MAT 08T22 Washington, D.C. 20360		13. NUMBER OF PAGES 52	
		15. SECURITY CLASS. (of this report) UNCLASSIFIED	
16. DISTRIBUTION STATEMENT (of this Report) APPROVED FOR PUBLIC RELEASE: DISTRIBUTION UNLIMITED 6-2-1-11		15a. DECLASSIFICATION/DOWNGRADING SCHEDULE	
17. DISTRIBUTION STATEMENT (of the abstract entered in Block 20, if different from Report)			
18. SUPPLEMENTARY NOTES			
19. KEY WORDS (Continue on reverse side if necessary and identify by block number) Circulation Control Boundary Layer Control High-Lift Systems Two-Dimensional Aerodynamics Supercritical Airfoil STOL Aircraft			
20. ABSTRACT (Continue on reverse side if necessary and identify by block number) Excellent high-lift and cruise performance of a small, round, fixed circulation control wing (CCW) trailing edge fitted to a supercritical airfoil has been confirmed by subsonic wind tunnel investigations. This fixed-trailing-edge blown high-lift airfoil generates a negligible subsonic cruise drag penalty, but can generate a section lift coefficient near 7.0. This configuration is a significant improvement over the flight-proven (Continued on reverse side)			

6

10

17

11

12 54

SEP 20 1981

A

→ next page

787695

TABLE OF CONTENTS

	Page
LIST OF FIGURES	iii
LIST OF TABLES.	iv
NOTATION.	v
ABSTRACT.	1
ADMINISTRATIVE INFORMATION.	1
INTRODUCTION.	1
DESIGN CONSIDERATIONS	2
MODELS AND EXPERIMENTAL APPARATUS	4
MODELS	4
EXPERIMENTAL APPARATUS AND TECHNIQUE	4
RESULTS AND DISCUSSION.	5
EFFECTIVE INCIDENCE.	5
LIFT AUGMENTATION DUE TO BLOWING	6
LIFT VARIATION WITH INCIDENCE.	7
COMPARATIVE LIFT PERFORMANCE	8
DRAG DUE TO BLOWING AND INCIDENCE.	8
PITCHING MOMENT.	10
CONCLUSION AND RECOMMENDATIONS.	10
REFERENCES.	13

LIST OF FIGURES

1 - Proposed CCW + CC/USB STOL Aircraft.	17
2 - NASA 17-Percent-Thick Supercritical Airfoil Section.	18
3 - CCW/Supercritical Airfoil Model Geometries	19
4 - Effective Incidence Corrections.	20

	Page
5 - Lift Characteristics of the NACA 64A008.4/CCW Airfoil (A-6/CCW Wing-Fold Section)	21
6 - Lift as a Function of Blowing and Slot Height for the CCW/Supercritical Airfoils at $\alpha_g = 0$ Degrees and $q_{ncm} = 10$ PSF.	23
7 - Lift as a Function of Blowing Pressure Ratio for Configuration 5, $r = 0.219$ Inches	27
8 - Effect of Incidence Variation on Lift for Configuration 5, $r = 0.219$ Inches	28
9 - Comparative CCW Airfoil Lift Performance, $h = 0.028$ Inches	30
10 - Comparative CCW Airfoil Lift Performance, $h = 0.014$ Inches	31
11 - Comparative CCW Airfoil Lift Performance, $h/r = 0.032$	32
12 - Drag Characteristics of the NACA 64A008.4/CCW Airfoil (A-6/CCW Wing-Fold Section).	33
13 - Drag as a Function of Blowing and Slot Height for the CCW/Supercritical Airfoils at $\alpha_g = 0$ Degrees and $q_{nom} = 10$ PSF.	34
14 - Drag as a Function of Blowing and Incidence for Configuration 5, $r = 0.219$ Inches	38
15 - Drag Polars for CCW/Supercritical Configuration 5 ($r = 0.219$ Inches) at Low Blowing.	39
16 - Unblown Lift and Drag Comparisons as Functions of Reynolds Number at $\alpha_g = 0$ Degrees.	40
17 - Pitching-Moment Characteristics of the NACA 64A008.4/CCW Airfoil (A-6/CCW Wing-Fold Section).	41
18 - Pitching Moment as a Function of Blowing and Slot Height for the CCW/Supercritical Airfoils at $\alpha_g = 0$ Degrees and $q_{nom} = 10$ PSF	42
19 - Comparative CCW Airfoil Pitching Moment, $h = 0.014$ Inches.	46

LIST OF TABLES

1 - Baseline 17-Percent-Thick Supercritical Airfoil Coordinates.	15
2 - CCW/Supercritical Airfoil Trailing Edge Parameters	16

NOTATION

C_d	Section drag coefficient
C_l	Section lift coefficient
$C_{m_{c/4}}$	Section quarter-chord pitching moment coefficient relative to $x = 0.25 c'$
C_μ	Blowing momentum coefficient, $\dot{m}V_j/qc'$
c	Original airfoil chordlength, in.
c'	Effective airfoil chordlength, as increased by CCW trailing edge addition, in.
h	Blowing jet slot height, in.
\dot{m}	Blowing jet mass efflux, slugs/sec
P_D	Blowing total pressure, psfa
P_∞	Free-stream static pressure, psfa
q	Corrected free-stream dynamic pressure, psf
q_{nom}	Nominal free-stream dynamic pressure, psf
Re	Reynolds number based on effective chord c'
r	Trailing edge radius, in.
t_{TE}	Trailing edge thickness ($2r$ for CCW airfoils), in.
V_j	Isentropic jet velocity, ft/sec
x	Longitudinal distance from leading edge, in.
z	Vertical distance from original chordline, in.
α_{eff}	Effective angle of attack, corrected for induced effects, deg
α_g	Geometric angle of attack, deg

α_{stall} Stall angle of attack, deg
 δ_{flap} Flap deflection angle, deg
 δ_{slat} Leading edge slat deflection below chordline, deg
 Δ Chordlength change experienced in assembly, in.

ABSTRACT

Excellent high-lift and cruise performance of a small, round, fixed circulation control wing (CCW) trailing edge fitted to a supercritical airfoil has been confirmed by subsonic wind tunnel investigations. This fixed-trailing-edge, blown high lift airfoil generates a negligible subsonic cruise drag penalty, but can generate a section lift coefficient near 7.0. This configuration is a significant improvement over the flight-proven A-6/CCW airfoil that had similar lift performance, but had a large trailing edge requiring mechanization for transition to cruise flight. Further, the large leading edge radius of the supercritical airfoil allows operating at high lift over a moderate angle-of-attack range. These results imply the feasibility of a mono-element airfoil with no moving components required for high lift; the transition from the cruise to the high-lift configuration is accomplished by blowing from a fixed slot. The favorable characteristics of both the cruise and high-lift airfoils are retained without compromise to either.

ADMINISTRATIVE INFORMATION

The work reported herein was funded by Naval Material Command (MAT 08D4) under Program Element 62241N, Task Area ZF 41421001, DTNSRDC Work Unit 1660-608 and by Naval Air Systems Command (AIR 320D) under Program Element 62241N, Task Area WF 41421000, DTNSRDC Work Unit 1600-081. The original baseline 17-percent-thick supercritical airfoil model was contributed by NASA Langley Research Center (Code 3860). Model modification was conducted from June through August 1980, and the two-dimensional investigations were conducted in two series: August through October 1980, and January 1981.

INTRODUCTION

The circulation control wing (CCW) concept has recently been proven in flight demonstrations as a very effective yet mechanically simple high-lift system capable of significant short takeoff and landing (STOL) characteristics.^{1-3*} As applied to a typical fixed-wing aircraft, the concept employs engine bleed air blown tangentially over a rounded trailing edge to amplify the airfoil circulation and

*A complete listing of references is given on page 13.

thus its high lift capability. Typical two-dimensional CCW airfoil sections using blowing rates available from production engine compressor bleed have tripled the lift generation of the basic airfoil section with a conventional mechanical flap.^{1,4} The A-6/CCW flight demonstrator airfoil incorporated a state-of-the-art large trailing edge radius of 3.67 percent chord to guarantee a successful flight demonstration, but any operational use of this design would require mechanized retraction of the system into the wing to avoid a large cruise drag penalty. An alternative for minimizing this drag problem is to reduce the trailing edge size to the point where it incurs no base drag penalty relative to the conventional airfoil. An advanced CCW STOL aircraft has been postulated^{5,6} which employs a small round trailing edge and blowing plenum, both contained within the cruise airfoil contour (Figure 1). This is accomplished by taking advantage of the large aft thickness of a typical bluff trailing edge supercritical airfoil, and provides the potential for a no-moving-parts high-lift system which does not have to be retracted for cruise. The system converts from cruise to high lift merely by initiating blowing and additionally provides the good cruise benefits of the supercritical section as well as the availability of blowing for transonic maneuverability. A reduced-radius ($r = 0.021c$) CCW trailing edge applied to a sharp trailing edge NACA 64A-212 airfoil has been investigated and was found to be quite effective.⁴ However, a CCW/supercritical combination had not been investigated, nor had a round trailing edge small enough to be compatible with its aft contour. The purpose of the present investigations is to assess both the lifting capabilities and the unblown drag levels of a series of progressively smaller CCW trailing edges on a typical supercritical airfoil. The ultimate goal is to produce a single-element CCW/supercritical no-moving-parts airfoil with minimal lift loss relative to larger radius CCW airfoils, and minimal drag penalty relative to bluff trailing edge supercritical sections.

DESIGN CONSIDERATIONS

To accomplish the above goals, it was desired to combine a typical, proven supercritical section with a set of baseline CCW trailing edge parameters typical of the A-6/CCW aircraft, and then progressively reduce the trailing edge size until it was compatible with the supercritical airfoil aft contour. The NASA 17-percent-thick supercritical airfoil shown in Figure 2 was both wind-tunnel

tested^{7,8} and flight tested^{7,9}, and therefore has a suitable reference data base. As the section coordinates in Table 1 confirm, the airfoil thickness produces a large bluff leading edge radius of 4.28-percent chord, which is of such substantial size that the radius may substitute for a mechanical leading edge device and thus further simplify the high-lift configuration. To parametrically vary the model trailing edge geometry, the A-6/CCW design radius-to-chord ratio of 0.0367 was taken as a baseline reference value, halved to give $r/c' = 0.018$ and halved again to give $r/c' = 0.009$. The smallest trailing edge diameter ($0.0188c'$) is then slightly greater than twice the $0.008c'$ trailing edge thickness of the baseline supercritical airfoil. These model configurations are shown in Figure 3.

To make results directly comparable, a constant slot height ($h = 0.028$ in., $h/r = 0.032$) would produce the same relation between blowing pressure and momentum coefficient C_{μ} for all airfoils, but would increase the slot-height-to-radius ratio for the smaller radii (h/r up to 0.128). Because Reference 4 suggests that strongly attached Coanda flow is maintained for $0.01 \leq h/r \leq 0.05$ and effective jet turning and lift augmentation result from $0.02 \leq r/c \leq 0.05$, the reduced radius configurations will exceed these guidelines. The effects of this will be an important test result.

An alternate trailing edge was designed in case the small radius proved unable to yield large lift augmentation. By employing twice the radius but only half a cylinder, the $0.018/c'$ design thickness and tendency for attached flow are maintained; but Coanda turning is limited to the 96-deg arc which ends at the sharp trailing edge, if the trailing edge is to remain fixed. A very short chord blown flap is thus formed, and lift augmentation will be limited by the maximum flow turning of 96 deg. This geometry is referred to in the following discussion as the 96-deg circular arc configuration.

Because the test objective is a comparison of lift and drag results produced by variation in blowing parameters rather than airfoil incidence, most of the investigations were planned at a geometric incidence of $\alpha_g = 0$ deg. Thus no leading edge device was thought to be necessary, especially when considering the large leading edge radius of the supercritical airfoil. However, a limited series of data was taken over a range of incidence values to provide a preliminary evaluation of leading edge capability.

MODELS AND EXPERIMENTAL APPARATUS

MODELS

The model configurations shown in Figure 3 were constructed based on the design considerations discussed in the previous section and on the 23-in. chord, two-dimensional NASA 17-percent-thick supercritical airfoil model described in Figure 2 and Table 1. This supercritical airfoil model was made available by NASA Langley Research Center; additional details of this basic model are found in Reference 7, and subsonic aerodynamic characteristics are presented in References 7 and 8. The model lower aft surface was machined to provide an air supply plenum cavity. The plenum lower wall was interchangeable and supported the various trailing edge geometries as shown in Figure 3. The center of each of these radii was located vertically below the slot lip, which was located at the trailing edge of the original airfoil. (A small machining error put this lip at $x = 22.981$ in. instead of the intended 23.000 in.) The gap between this upper lip and the round trailing edges became the tangential blowing slot, and was adjustable in height by use of compression and jacking screws. The slot exit was thus a constant distance from the airfoil leading edge for all models. The effective chord c' is the sum of the original chord (now $x = 22.981$ in.), the trailing edge radius (r), and any slight trailing edge horizontal displacement (Δ) experienced in assembly. All reported force, moment, and blowing coefficients are based on c' , since this is considered to be the undeflected cruise reference chord of each airfoil. Table 2 lists the trailing edge parameters for these airfoils. Note that Configurations 3 and 5 are basically the same small radius configuration. After testing and disassembly of Configuration 3, it was noted that pressure tubing in the small plenum had partially blocked portions of the slot. This was corrected to allow a smooth internal plenum and an unobstructed entrance to the slot, and then was re-tested as Configuration 5.

EXPERIMENTAL APPARATUS AND TECHNIQUE

The 3-ft span two-dimensional models described were mounted between the 3- by 8-ft subsonic two-dimensional wall inserts installed in the DTNSRDC 8- by 10-ft subsonic tunnel.^{4,8} Lift and moment coefficients were obtained by numerical integration of surface static pressures near the midspan as recorded by a 144-port scanivalve system. The drag coefficient was obtained from integration of wake momentum deficit as measured on a fixed total head wake rake spanning nearly 8 ft

from floor to ceiling. Model installation, test apparatus and technique, data reduction and corrections, and monitoring of tunnel two-dimensionality were all conducted as reported in Reference 4 (Appendix A) and Reference 8. Photographs of the test setup employed are also included in Reference 4. The momentum coefficient C_{μ} was calculated as $\dot{m}V_j/(qc')$, where \dot{m} is the mass flow per unit slot span as measured by venturimeter, and V_j is the calculated isentropic jet velocity calculated using the equation in Reference 4. One difference in test techniques from the Reference 4 procedures is that the tangential wall blowing slots intended to retain two-dimensionality from wall to wall were not employed because a failure in the lip of one slot made them unequal and ineffective. Thus, the effective angle of attack for all data will be less than the geometrically set value due to the presence of some three-dimensional tip (wall) effects and the resulting downwash.

RESULTS AND DISCUSSION

Experimental investigations were conducted in approximately the order of the Table 2 listing, where duct pressure and then slot height were varied for each configuration at a geometric incidence of 0 deg. Additional variations were made in Reynolds number and angle of attack before conversion to the next trailing edge configuration. The following discussion concentrates mainly on the effects of these variations and the resulting performance of the four trailing edge geometries.

EFFECTIVE INCIDENCE

Because the tangential wall blowing system normally used to enhance test section two-dimensionality was inoperative for these investigations, spanwise static pressure distributions across the model from wall to wall were recorded and compared to those from the two-dimensional investigations of References 1, 3, and 4. These present variations were found to be at least as uniform as those previously obtained. Therefore, the incidence corrections due to induced angle of attack as applied in the previous tests should be applicable here also. These corrections are presented in Figure 4. As lift coefficient increases, effective incidence is reduced due to increased vorticity at the model-wall junction and the resulting induced downwash angles along the model span. The effective incidence c_{eff} is thus the corrected true angle of attack at which the airfoil midspan (static pressure tap location) is operating, and Figure 4 may be employed to obtain those values.

However, in order to make comparisons at the same nominal incidence, the airfoil characteristics that follow are presented for constant values of geometric incidence α_g .

LIFT AUGMENTATION DUE TO BLOWING

Section lift is presented in Figure 5 as a function of momentum coefficient and incidence for the NACA 64A008.4/CCW airfoil section (References 1 and 3) to allow comparisons to the lift performance of a state-of-the-art CCW airfoil. This is the airfoil at the wing fold-line on the A-6/CCW flight demonstrator aircraft; the geometric parameters shown thus represent flight-proven values capable of high lift and significant STOL performance^{2,3}. The drawing of this airfoil in Figure 5a shows the relative size of the rounded trailing edge and emphasizes the need to reduce that geometry to the smaller trailing edges of Figure 3. For these four different trailing edge configurations applied to the supercritical airfoil, section lift coefficients are presented in Figure 6 as functions of momentum coefficient and slot height at 0-deg incidence and a nominal free-stream dynamic pressure of 10 psf ($R_e = 1.2 \times 10^6$). For all three of the full circular trailing edges (Configurations 1, 2, and 5), an increase in slot height yielded increased lift at constant C_{μ} , until some upper limit on slot height was reached. For the 0.875-in. and 0.438-in. trailing edge radius configurations, the largest slot heights caused a reduction in lift for all values of C_{μ} ; but for the small 0.219-in. radius trailing edge, larger slot heights produced larger lift until a certain value of C_{μ} was reached, after which lift dropped significantly. This was found to be a function of the pressure ratio effect on the blowing jet attachment which could be sustained by the small radius. (See Reference 10 for a discussion of jet detachment at higher pressures for small radii.) In Figure 7, it is confirmed that for each slot height, a pressure ratio exists beyond which lift reduces with increased blowing on the small radius airfoil. The same effect occurs for the 0.438-in. radius of Configuration 2, but only for the large $h = 0.056$ in. Since, for both of these airfoils, these limiting pressure ratios are reached at lower C_{μ} values as q is increased, it was decided to run the majority of these investigations at $q = 10$ psf and thus extend the attached-flow C_{μ} range. Figure 6d shows flow detachment for $h = 0.014$ in. occurring at $C_{\mu} \approx 0.17$ when $q = 25$ psf, but not until $C_{\mu} \approx 0.45$ for $q = 10$ psf. The Figure 7 data emphasize the effectiveness of the small trailing edge airfoil when run at the low pressure ratio (and

corresponding higher slot heights) characteristic of powering the airfoil with turbofan bypass airflow.

Figure 6c offers an alternative to the completely round trailing edge, where the circular arc trailing edge of Configuration 4 ends in a sharp corner at approximately 96 deg from the slot. This fixes the jet separation point and minimizes the effects of slot height change. It also produces considerably less lift than the full round configurations, but seems to assure jet attachment at much higher pressure ratios and C_{μ} values. The performance of this airfoil closely resembles the characteristic jet flap, as is also seen by its drag characteristics and considerable thrust recovery.

LIFT VARIATION WITH INCIDENCE

While all of the configurations were investigated at 0 deg and several other discrete angles of attack for comparison, the small radius Configuration 5 airfoil was run over a geometric angle-of-attack range from -5 deg to +15 deg. These lift data for the 0.014-in. slot height are presented as a function of blowing at constant incidence in Figure 8a, and are crossplotted as the more conventional C_{μ} versus α at constant C_{μ} in Figure 8b. These plots may be compared directly to the data of the state-of-the-art A-6/CCW airfoil of Figure 5, which was run at a larger slot height and Reynolds number than Configuration 5. Two trends are noticeable. First, the lift on the CCW/supercritical airfoil, with a radius only 25 percent as large as the A-6/CCW airfoil, is slightly greater than that airfoil at lower α and C_{μ} , since the A-6 slat imparts a download under these conditions. Second, the undeflected bulbous nose of the supercritical airfoil provides the same or better leading edge performance as the A-6 37.5 deg slat, yielding almost identical stall angles at any given C_{μ} .

The apparent deficits in certain of the lift curves (primarily for $6 \text{ deg} \leq \alpha_g \leq 12 \text{ deg}$ and $C_{\mu} < 0.20$) are due to flow separation on the supercritical airfoil aft upper surface, between the crest and the slot. (This condition is discussed in detail in Reference 11.) The separated flow is re-entrained at higher C_{μ} , and the deficits disappear.

COMPARATIVE LIFT PERFORMANCE

In Figure 9, the four supercritical airfoil configurations are compared with each other at the same slot height ($h = 0.028$ in.), Reynolds number ($R_e \doteq 1.2 \times 10^6$, $q \doteq 10$ psf), and incidence ($\alpha_g = 0$ deg), and to the A-6/CCW at a similar slot height ($h = 0.027$ in.) but at a higher Reynolds number (1.9×10^6 , $q = 25$ psf). Reduction in trailing edge radius on the CCW/supercritical airfoil tends to only slightly reduce C_{L_2} . At a typical C_{μ} of 0.25, the small radius configuration generates only 5 percent less lift than Configuration 1, which has a radius four times as large. In Figure 10, for $h = 0.014$ in. instead of 0.028 in., the reduction in lift is 7 percent. However, all three round trailing edges perform better than the A-6/CCW airfoil at $\alpha_g = 0$ deg, probably because of the slot download and the resulting lift loss. The basic 17-percent supercritical airfoil without blowing (Reference 7) generates only $C_{L_2} = 0.4$ at this incidence. The 96-deg circular arc airfoil generates less circulation lift than the full round trailing edges due to the fixed jet separation point locations and limited flow turning.

The Figure 10 data for the reduced slot height show similar trends to Figure 9. However, lift levels are slightly lower, and the small radius maintains jet attachment to considerably higher C_{L_2} and C_{μ} values than for $h = 0.028$ in. A comparison of these configurations is made in Figure 11 for a constant slot-height-to-radius ratio, $h/r = 0.032$. The constant h/r forces smaller slot heights on the smaller radius airfoils, and thus the reduction in lift for the small radius is increased somewhat, as emphasized in Figure 7.

DRAG DUE TO BLOWING AND INCIDENCE

Two-dimensional drag coefficients obtained from wake rake pressure integrations are presented in Figure 12 for the A-6/CCW airfoil and in Figure 13 for the four CCW/Supercritical configurations at $\alpha_g = 0$ deg. Whereas some scatter exists in these data (just as it did in the basic airfoil drag measurements of Reference 7), some obvious trends can be detected. Initiation of blowing causes an immediate reduction in measured drag coefficient because, at these low jet turning conditions, the jet momentum is recovered as thrust and the wake momentum deficit is diminished. For the 96-deg circular arc (Figure 13c), this trend of reducing drag by increasing C_{μ} continues throughout the entire range of blowing tested; however, for the full round trailing edges, the jet continues to turn as C_{μ} increases. As a result, thrust recovery diminishes, a larger viscous wake is generated, and drag

begins to increase. This increase in drag is also due to the increased profile drag caused by large negative pressure regions over the round trailing edge, and thus larger drag values occur for the larger radii configurations at higher blowing.

Drag variation with incidence is presented in Figure 14 for the small trailing edge airfoil at $h = 0.014$ in. With the exception of the aft flow separation regimes at $\alpha_g = 9$ deg and 12 deg, drag levels are lower at all incidences than the larger radius A-6/CCW airfoil of Figure 12 (at a higher Reynolds number), and significant regions of negative drag (thrust recovery) are present. The reduced size bluff trailing edge thus can significantly increase the efficiency (blown ℓ/d) of CCW airfoils.

Drag polars for the small radius airfoil at low blowing values ($C_\mu \leq 0.05$) are compared in Figure 15 with the baseline 17-percent supercritical airfoil operating at a higher Reynolds number. The drag values of the baseline airfoil are slightly lower than those of the CCW/supercritical airfoil with no blowing ($\Delta C_d = 0.0006$ at $\alpha_g = 0$ deg and $R_e = 2 \times 10^6$); however, the drag of the blown airfoil can be reduced to that of the baseline airfoil by blowing at $C_\mu \leq 0.005$ for $\alpha_g \leq 9$ deg. Additional blowing will reduce the drag even further. Thus, the high-lift device of the CCW airfoil may be left exposed for cruise conditions with essentially no drag penalty.

Reynolds number effects on the large and small radius CCW airfoils are shown in Figure 16. Lift coefficient remains constant over the range evaluated. Drag coefficient reduces noticeably with Reynolds number for the large radius, but rather insignificantly for the small radius. For both radii, C_d appears constant for $R_e \geq 2 \times 10^6$. A sharp trailing edge NACA 64₃-418 airfoil (from Reference 12) is included here for comparison, as is the baseline NASA supercritical airfoil. At $R_e = 2 \times 10^6$, the unblown lift and drag values at $\alpha_g = 0$ deg are:

<u>Airfoil</u>	<u>C_d</u>	<u>C_ℓ</u>
64 ₃ -418 ($R_e = 3 \times 10^6$)	0.0061	0.330
Baseline supercritical	0.0084	0.400
Small CCW, $r = 0.219$ in.	0.0090	0.455
Large CCW, $r = 0.875$ in.	0.0183	0.671

PITCHING MOMENT

As is typical of most blown airfoils, the increased suction region near the trailing edge blowing source generates increased nose-down pitching moment, as is verified in Figure 17 for the A-6/CCW airfoil section. Increase in incidence adds leading edge suction regions which counteract those at the trailing edge and thus reduce the nose-down moment. This nose-down pitch was trimmable with modification to the existing stabilizer on the A-6/CCW.¹⁻³ The enlarged tail area employed could have been reduced in size due to the favorable effects of engine thrust on the tail. Quarter-chord pitching moments at 0-deg incidence and $q = 10$ psf for the four CCW/supercritical configurations are presented in Figure 18. These configurations generate similar trends to the A-6 airfoil. As the slope of the C_l versus C_{μ} curve decreases, the pitching moment slope reduces as well, or pitch-up occurs in the case of flow separation. For $C_{\mu} \leq 0.25$, the supercritical sections generate less nose-down pitch than the A-6/CCW airfoil (Figure 19). This is probably due to greater vertical suction components on the undeflected supercritical leading edge radius.

CONCLUSIONS AND RECOMMENDATIONS

Circulation control wing technology was applied to a NASA 17-percent-thick supercritical airfoil. Circular trailing edges of three different radii were evaluated: a large radius comparable to the A-6/CCW aircraft, a small radius approximately twice the thickness of the supercritical airfoil trailing edge, and a radius in between these two. A fourth configuration was developed using 96 deg of circular arc on the intermediate size radius. The results of subsonic two-dimensional wind tunnel investigations indicate the small trailing edge size can be applied to a supercritical airfoil without degrading CCW performance. The following conclusions resulted from these investigations.

- Reduction in trailing edge radius size from a state-of-the-art value (0.0366c') to 25 percent that size (0.0094c') results in lift losses of only 5 to 7 percent at zero incidence, depending on C_{μ} and slot height. Lift coefficients greater than 5.5 were generated at $C_{\mu} \leq 0.25$ and $\alpha_g = 0$ deg for both configurations.

- All CCW/supercritical configurations with full round trailing edges produced greater lift at $\alpha_g = 0$ deg than the A-6/CCW airfoil at the same slot height due to the absence of download which existed on the leading edge slot of the flight-proven airfoil.

- The large bulbous nondeflecting leading edge of the supercritical airfoil provides flow attachment capability the same as or better than the A-6/CCW's 37.5-deg leading edge slot, generating almost identical stall angles at the same C_{μ} but at a lower Reynolds number. A C_L near 7 at $C_{\mu} = 0.4$ and $\alpha_g = 10$ deg was generated by the small radius CCW/supercritical airfoil.

- The CCW/supercritical configurations performed better at larger slot heights as long as certain pressure ratio limits were not exceeded for the smaller radii. This makes them especially compatible with the low pressure, high mass flow characteristics of turbofan bypass fan air.

- The reduced jet turning of the 96-deg circular arc configuration reduced lift generation but increased thrust recovery and drag reduction while operating apparently unrestrained by the limits due to higher pressure ratio.

- For the fully rounded trailing edge configurations, drag initially was reduced at low C_{μ} and then began to rise at higher blowing due to trailing edge suction and viscous mixing. The rise did not occur on the 96-deg arc configuration.

- Base drag was minimized by the small trailing edge radius so that unblown C_D was essentially the same as the baseline 17-percent supercritical section. Drag could be further reduced on the small radius CCW airfoil to less than that of the baseline airfoil by minimal blowing ($C_{\mu} \leq 0.005$).

- Nose-down pitching moments for all supercritical blown configurations were less than the flight-trimmable A-6/CCW airfoil for $C_{\mu} \leq 0.25$.

These results suggest the strong possibility of a combined cruise and high-lift mono-element airfoil, where the favorable characteristics of each airfoil are retained without compromising the other, and no mechanical moving parts are required to transition from one mode to the other. The small radius CCW fits almost within the existing supercritical airfoil aft contour. Negligible drag penalties occur in the cruise mode from leaving exposed a system that can generate a section lift coefficient greater than 6.5 at $\alpha_g = 0$ deg in the high-lift mode. The supercritical airfoil thick contour can provide the already proven favorable

transonic cruise performance, and its thick leading edge provides a very effective nondeflecting anti-separation device to compliment the high circulation properties of the round trailing edges. The remaining unknown is the effect of the nonretracting small trailing edge on the drag characteristics of the airfoil in high subsonic and transonic flow. It is thus recommended that a transonic two-dimensional investigation be conducted to determine the unblown and low-blowing performance of the combined CCW/supercritical configuration.

REFERENCES

1. Englar, R.J. et al., "Design of the Circulation Control Wing STOL Demonstrator Aircraft," AIAA Paper No. 79-1842 presented at the AIAA Aircraft Systems and Technology Meeting, New York (Aug 1979). Republished in AIAA Journal of Aircraft, Vol. 18, No. 1, pp. 51-58 (Jan 1981).
2. Pugliese, A.J. and R.J. Englar, "Flight Testing the Circulation Control Wing," AIAA Paper No. 79-1791 presented at AIAA Aircraft Systems and Technology Meeting, New York (Aug 1979).
3. Englar, R.J., "Development of the A-6/Circulation Control Wing Flight Demonstration Configuration," DTNSRDC Report ASED-79/01 (Jan 1979).
4. Englar, R.J., "Subsonic Two-Dimensional Wind Tunnel Investigations of the High Lift Capability of Circulation Control Wing Sections," DTNSRDC Report ASED-274 (Apr 1975).
5. Nichols, J.H., Jr., and R.J. Englar, "Advanced Circulation Control Wing System for Navy STOL Aircraft," AIAA Paper No. 80-1825 presented at the AIAA Aircraft Systems Meeting, Anaheim, California (4-6 Aug 1980).
6. Nichols, J.H., Jr., et al., "Experimental Development of an Advanced Circulation Control Wing System for Navy STOL Aircraft," AIAA Paper No. 81-0151 presented at the AIAA 19th Aerospace Sciences Meeting, St. Louis (12-15 Jan 1981).
7. McGhee, R.H. and G.H. Bingham, "Low-Speed Aerodynamic Characteristics of a 17-Percent Thick Supercritical Airfoil Section, Including a Comparison Between Wind-Tunnel and Flight Data," NASA TM X-2571 (Jul 1972).
8. Englar, R.J. and J. Ottensoser, "Calibration of Some Subsonic Wind Tunnel Inserts for Two-Dimensional Airfoil Experiments," NSRDC Report ASED AL-275 (Sep 1972).
9. Palmer, W.E. et al., "Flight and Wind-Tunnel Evaluation of a 17% Thick Supercritical Airfoil on a T-2C Airplane," Vol. I and II, North American Rockwell Corp. Report NR71H-150 (Jul 1971).
10. Englar, R.J., "Experimental Investigation of the High Velocity Coanda Wall Jet Applied to Bluff Trailing Edge Circulation Control Airfoils," DTNSRDC Report 4708 (Sep 1975).

11. Englar, R.J., "Two-Dimensional Subsonic Wind Tunnel Tests of a Cambered 30-Percent Thick Circulation Control Airfoil," NSRDC Report ASED AL-201 (May 1972).

12. Abbott, I.H. and A.E. Von Doenhoff, "Theory of Wing Sections," Dover Publications, New York (1959).

TABLE 1 - BASELINE 17-PERCENT-THICK SUPERCRITICAL AIRFOIL COORDINATES
(from Reference 7)

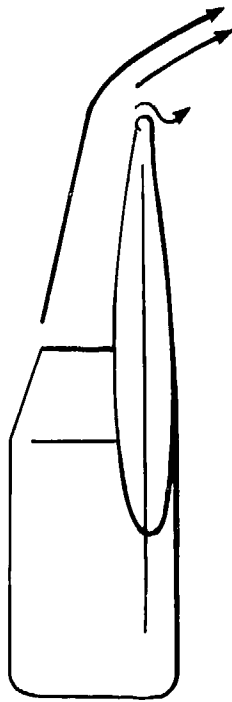
[Leading-edge radius: 0.0428c; c = 59.42 cm (23 in.)]

x/c	(z/c) _{upper}	(z/c) _{lower}
0.0	0.000	0.000
.0125	.0304	-.030
.0250	.0401	-.0408
.0375	.0469	-.048
.0500	.0519	-.0533
.075	.0595	-.0611
.100	.0652	-.0664
.125	.06963	-.0704
.150	.07325	-.0735
.175	.07625	-.0760
.200	.07890	-.0779
.250	.0837	-.0807
.300	.0863	-.0819
.350	.08825	-.0820
.400	.0891	-.0810
.450	.08893	-.0786
.500	.08783	-.0748
.550	.08568	-.0690
.575	.08423	-.0652
.600	.08248	-.0607
.625	.08043	-.0554
.650	.07811	-.0495
.675	.07541	-.0431
.700	.07233	-.0366
.725	.06881	-.0301
.750	.06476	-.0240
.775	.0602	-.0184
.800	.0553	-.0134
.825	.0499	-.0093
.850	.0440	-.0060
.875	.0376	-.0036
.900	.0308	-.0021
.925	.0236	-.0017
.95	.0160	-.0025
.975	.0081	-.0044
1.000	.00	-.0080

TABLE 2 - CCW/SUPERCritical AIRFOIL TRAILING EDGE PARAMETERS

($c = 23.000$ in., $x_{slot} = 22.981$ in., $\Delta =$ aft shift in T. E. at assembly)

Configuration	$r,$ in.	$c' =$ $x_{slot} + r + \Delta$	r/c'	$h,$	h/r	h/c'	x/c'_{slot}
1	0.875 ↓	23.886 ↓	0.03663 ↓	0.028	0.032	0.001172	0.96211 ↓
				0.014	0.016	0.000586	
				0.007	0.008	0.000293	
				0.056	0.064	0.002344	
2	0.438 ↓	23.474 ↓	0.01864 ↓	0.028	0.064	0.001193	0.97900 ↓
				0.014	0.032	0.000596	
				0.007	0.016	0.000298	
				0.056	0.128	0.002386	
3	0.219 ↓	23.224 ↓	0.009421 ↓	0.028	0.128	0.001206	0.98954 ↓
				0.014	0.064	0.000603	
				0.007	0.032	0.000301	
				0.021	0.096	0.000904	
4 (96-deg circular arc)	0.438 ↓	23.419 ↓	0.018682 ↓	0.014	0.032	0.000598	0.98130 ↓
				0.028	0.064	0.001196	
				0.056	0.128	0.002391	
				0.007	0.016	0.000299	
5 (3 with reworked plenum)	0.219 ↓	23.210 ↓	0.009427 ↓	0.014	0.064	0.000603	0.99013 ↓
				0.021	0.096	0.000905	
				0.028	0.128	0.001206	
				0.007	0.032	0.000302	



INBOARD: CIRCULATION CONTROL
WING/THRUST DEFLECTOR



OUTBOARD: CIRCULATION CONTROL
WING ON SUPERCritical AIRFOIL



Figure 1 - Proposed CCW + CC/USB STOL Aircraft

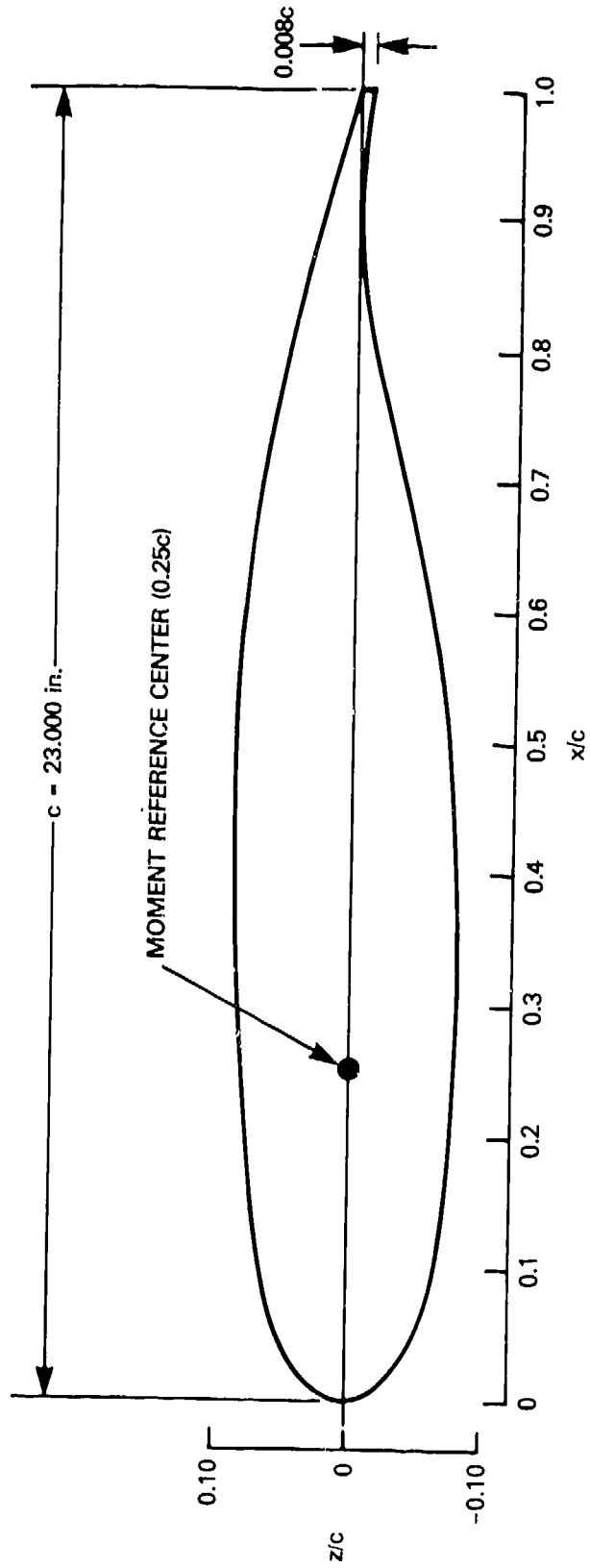
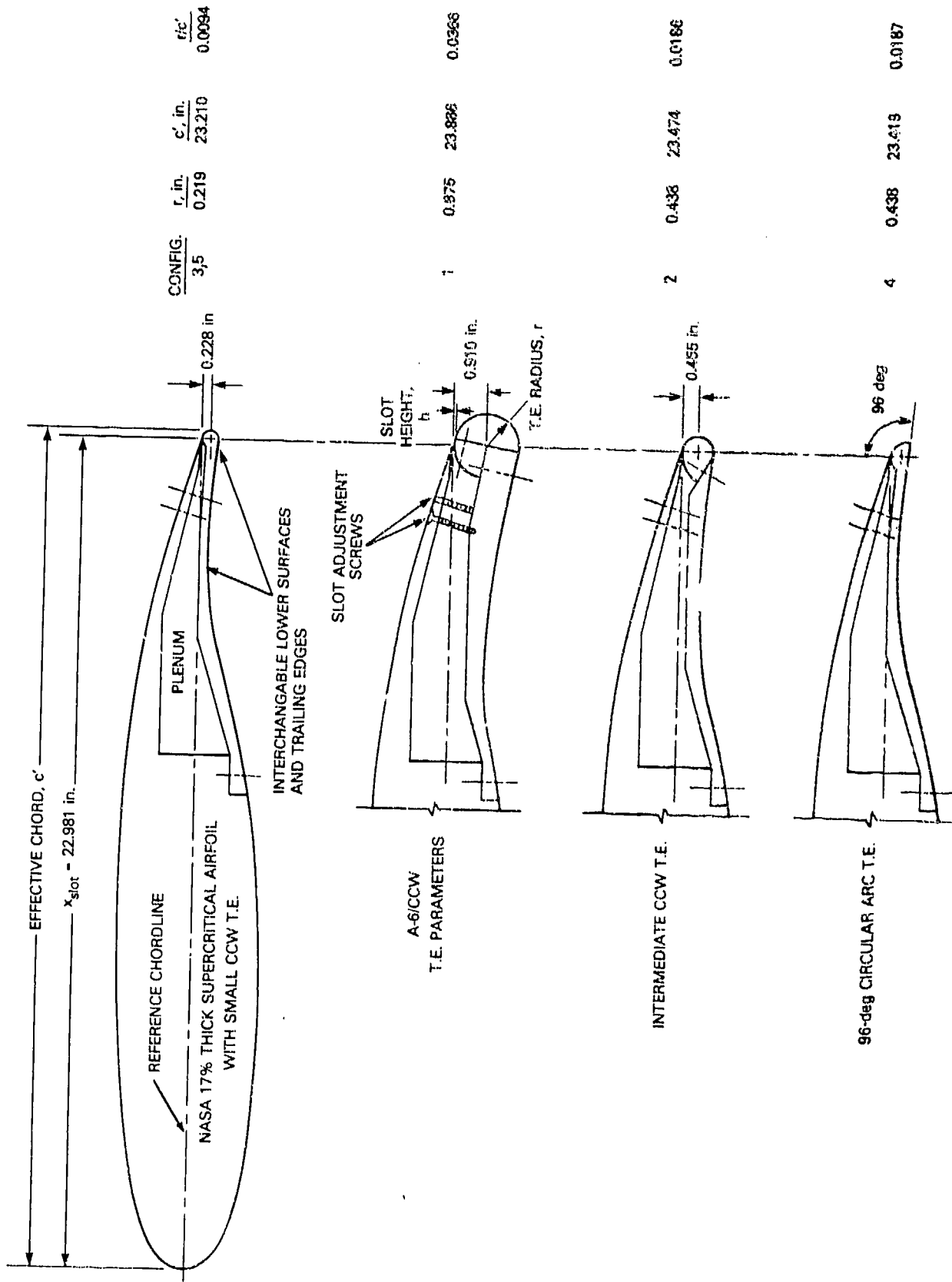


Figure 2 - NASA 17-Percent-Thick Supercritical Airfoil Section
(from Reference 7)



NOTE: (1) ORIGINAL CHORD $c = 23.000 \text{ in.}$

(2) SLOT HEIGHT SHOWN CLOSED ON ALL CONFIGS. EXCEPT NO. 1

Figure 3 - CCW/Supercritical Airfoil Model Geometries

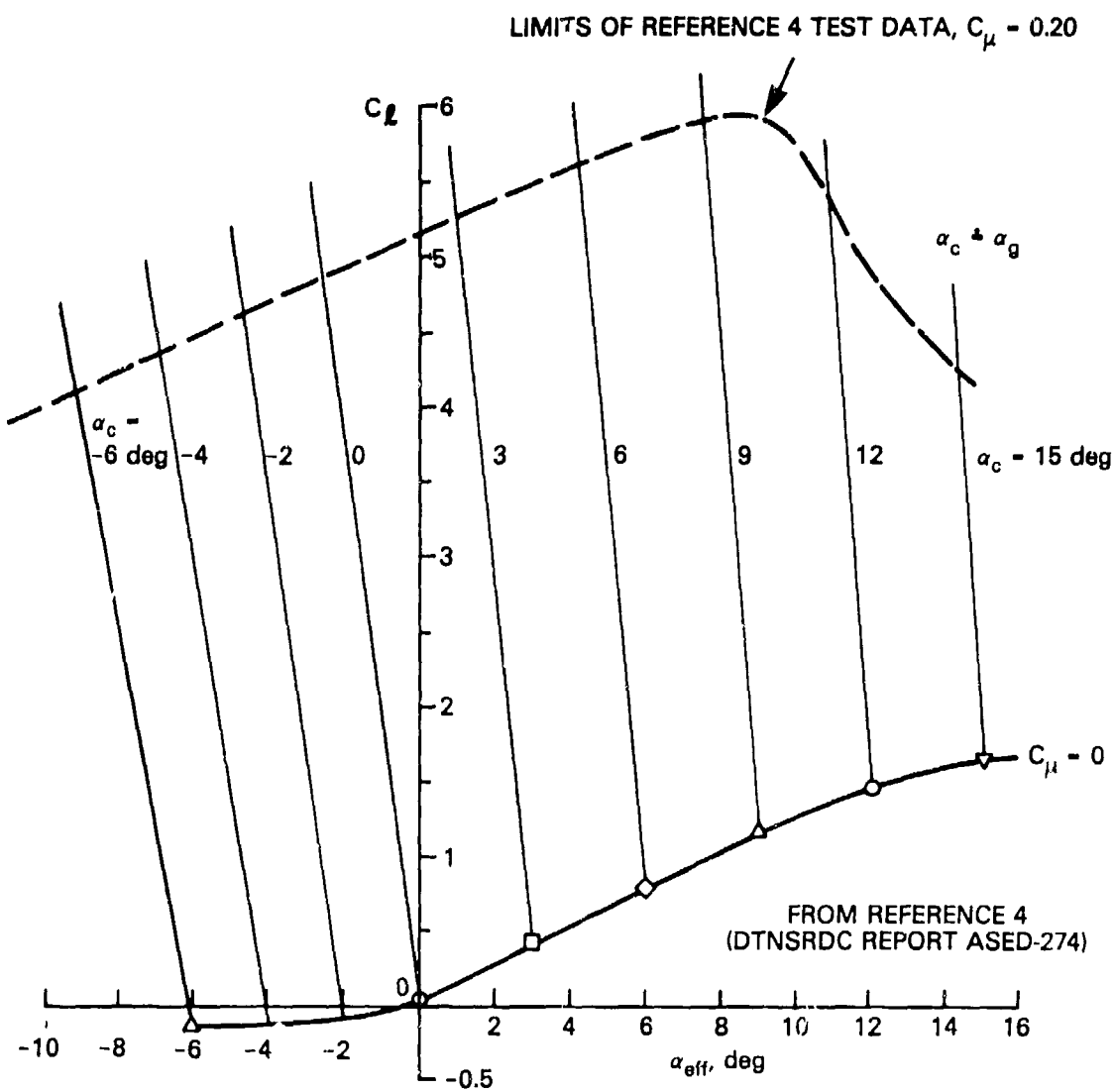


Figure 4 - Effective Incidence Corrections

Figure 5 - Lift Characteristics of the NACA 64A008.4/CCW Airfoil
(A-6/CCW Wing-Fold Section)

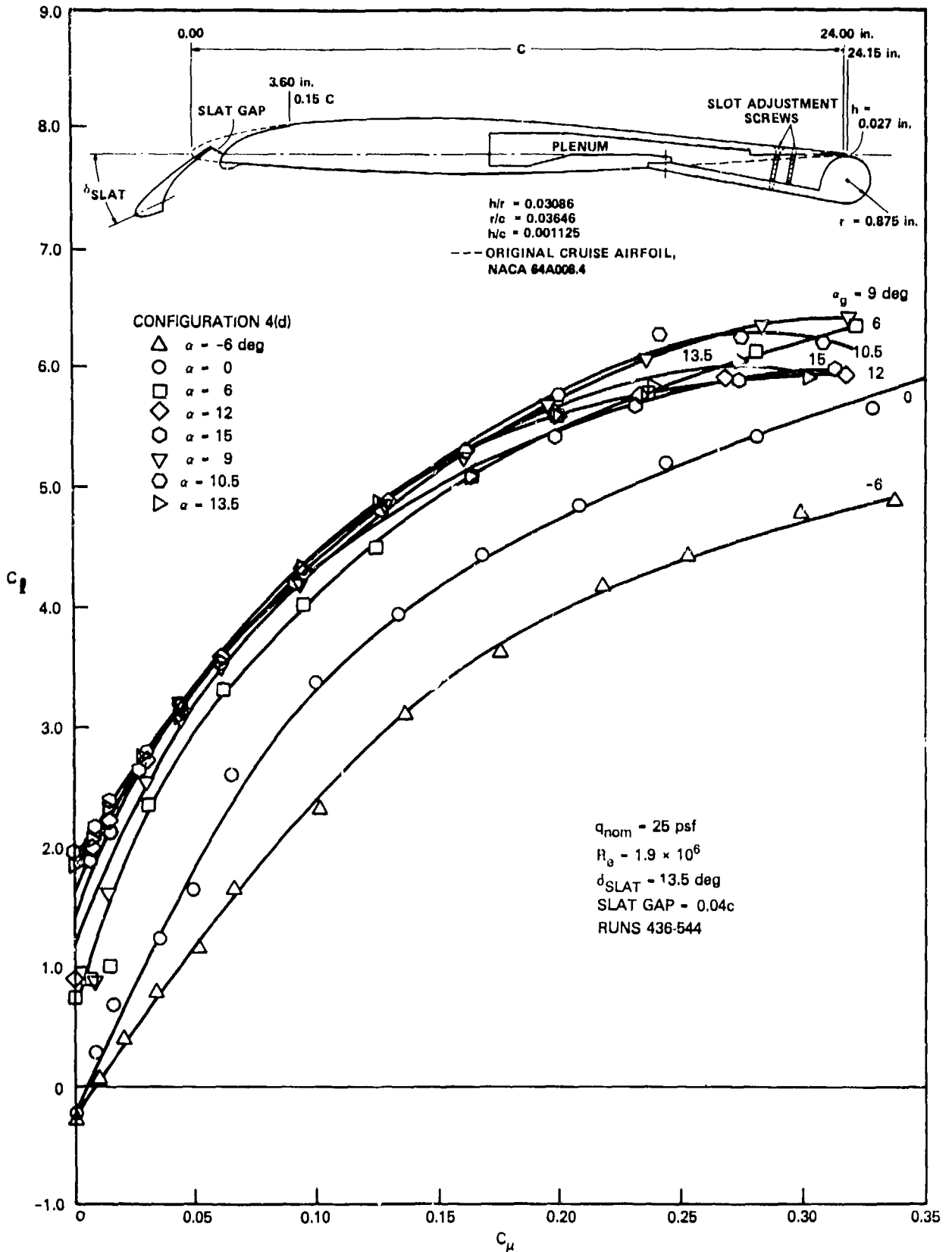


Figure 5a - Lift as a Function of Blowing

Figure 5 (Continued)

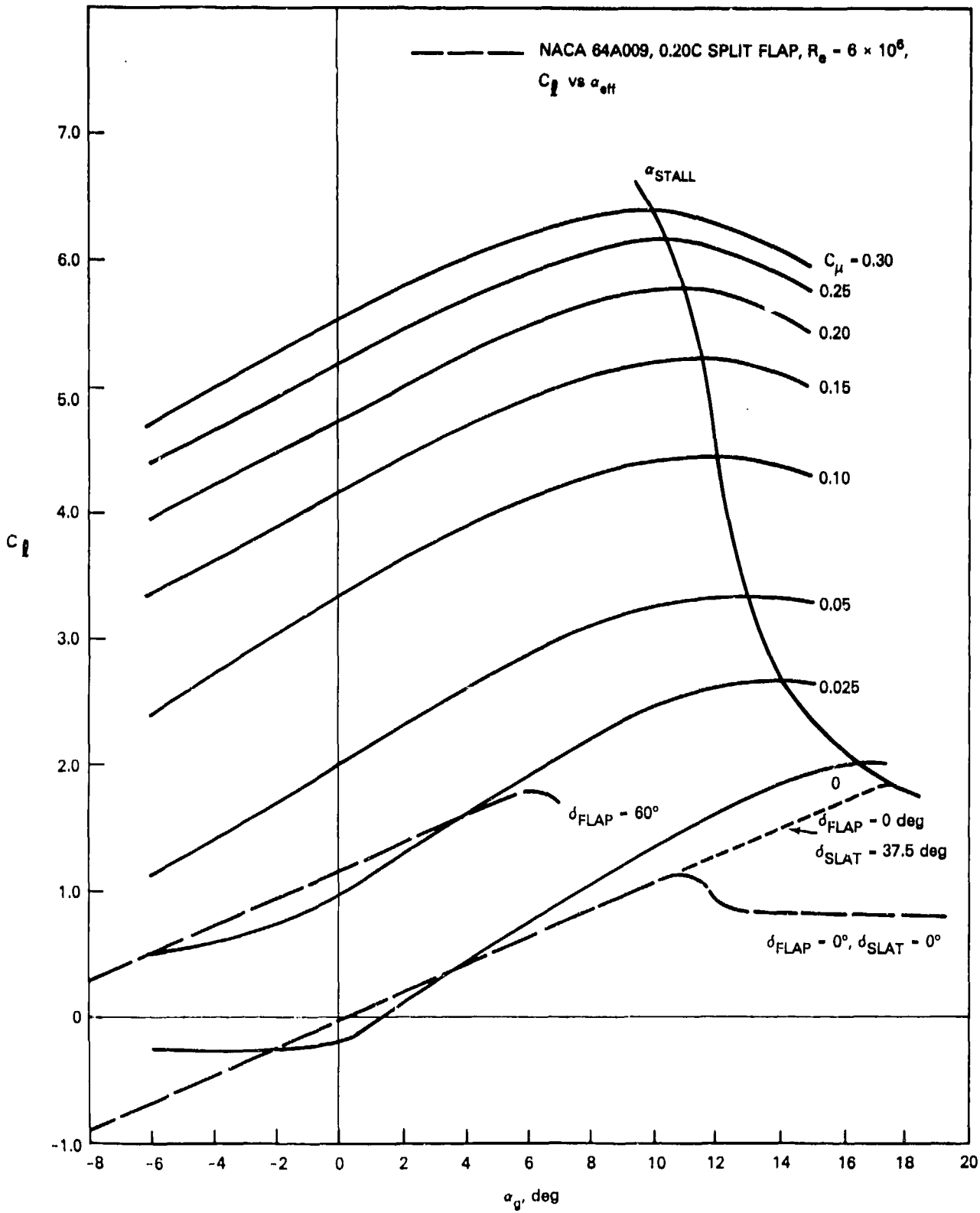


Figure 5b - Lift as a Function of Incidence

Figure 6 - Lift as a Function of Blowing and Slot Height for the CCW/Supercritical Airfoils at $\alpha_g = 0$ Degrees and $q_{nom} = 10$ PSF

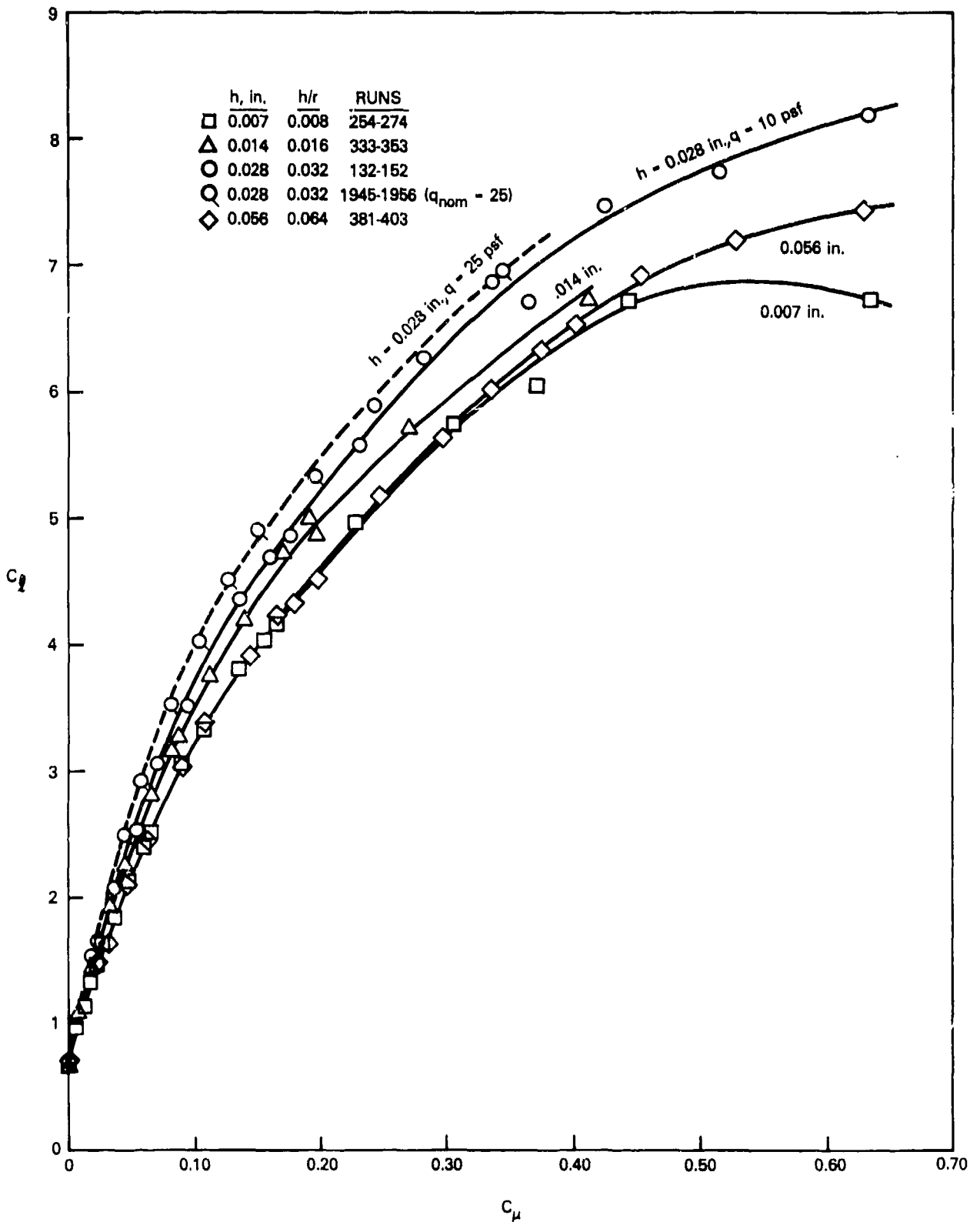


Figure 6a - Configuration 1, $r = 0.875$ Inches, $r/c' = 0.0366$

Figure 6 (Continued)

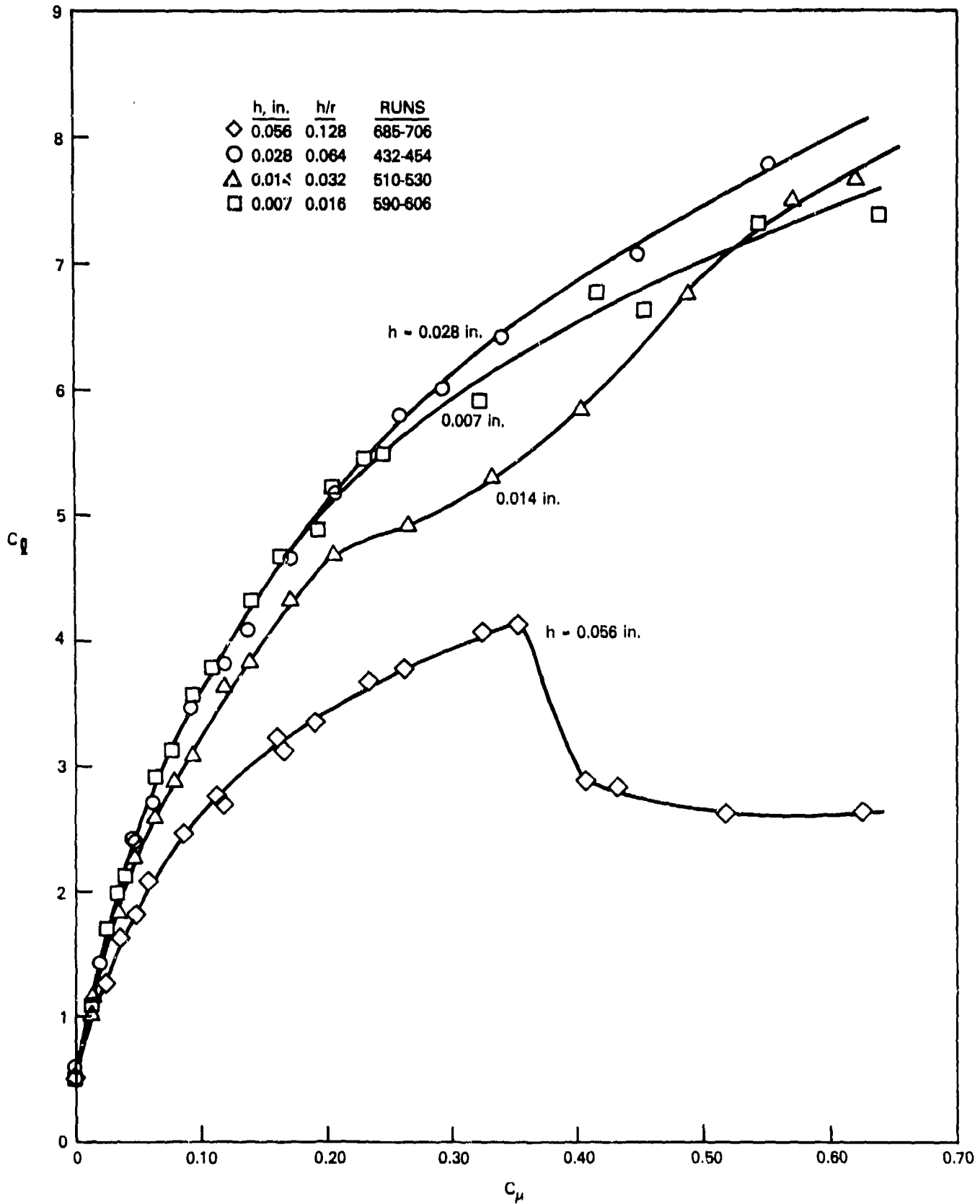


Figure 6b - Configuration 2, $r = 0.438$ Inches, $r/c' = 0.0186$

Figure 6 (Continued)

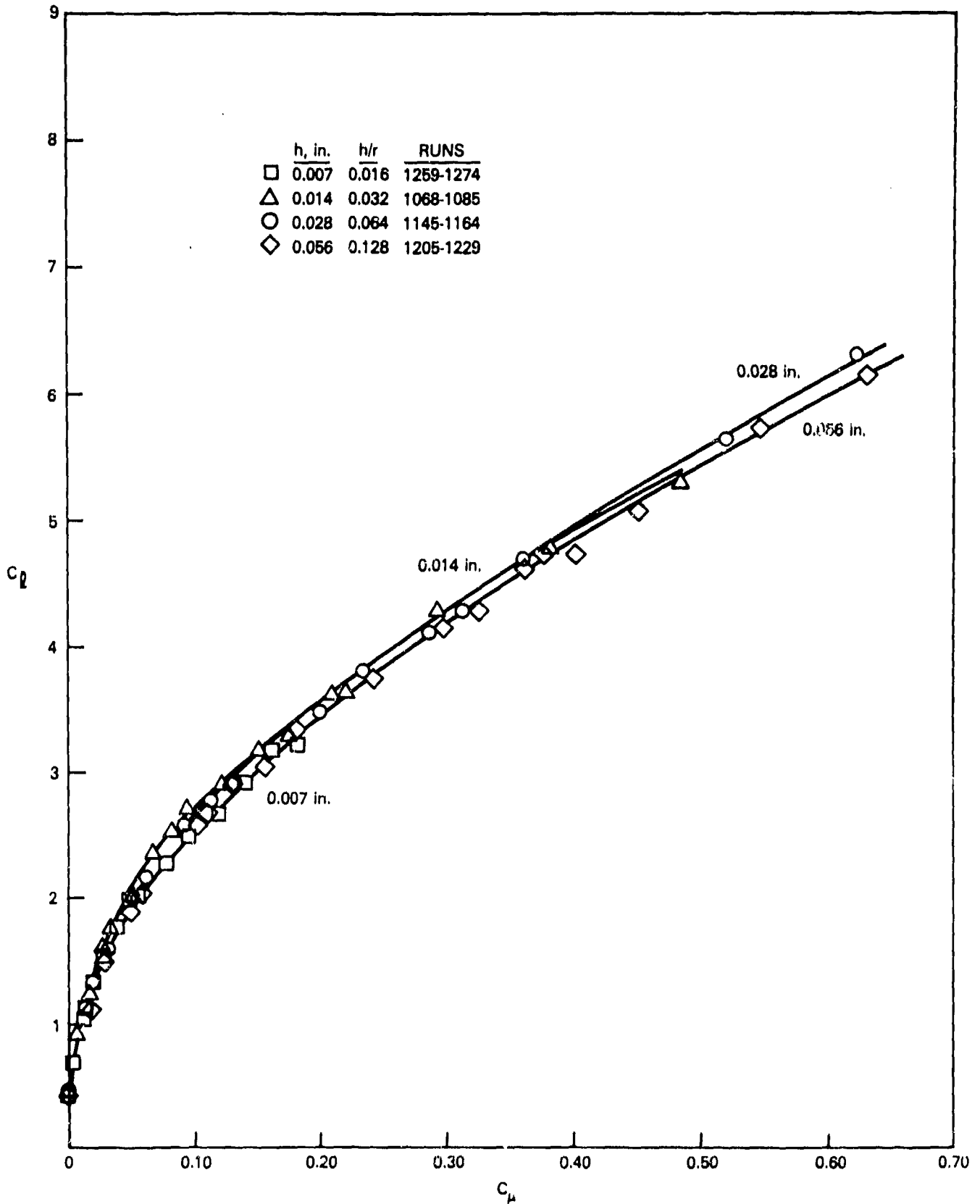


Figure 6c - Configuration 4, 96-Degree Circular Arc,
 $r = 0.438$ Inches, $r/c' = 0.0187$

Figure 6 (Continued)

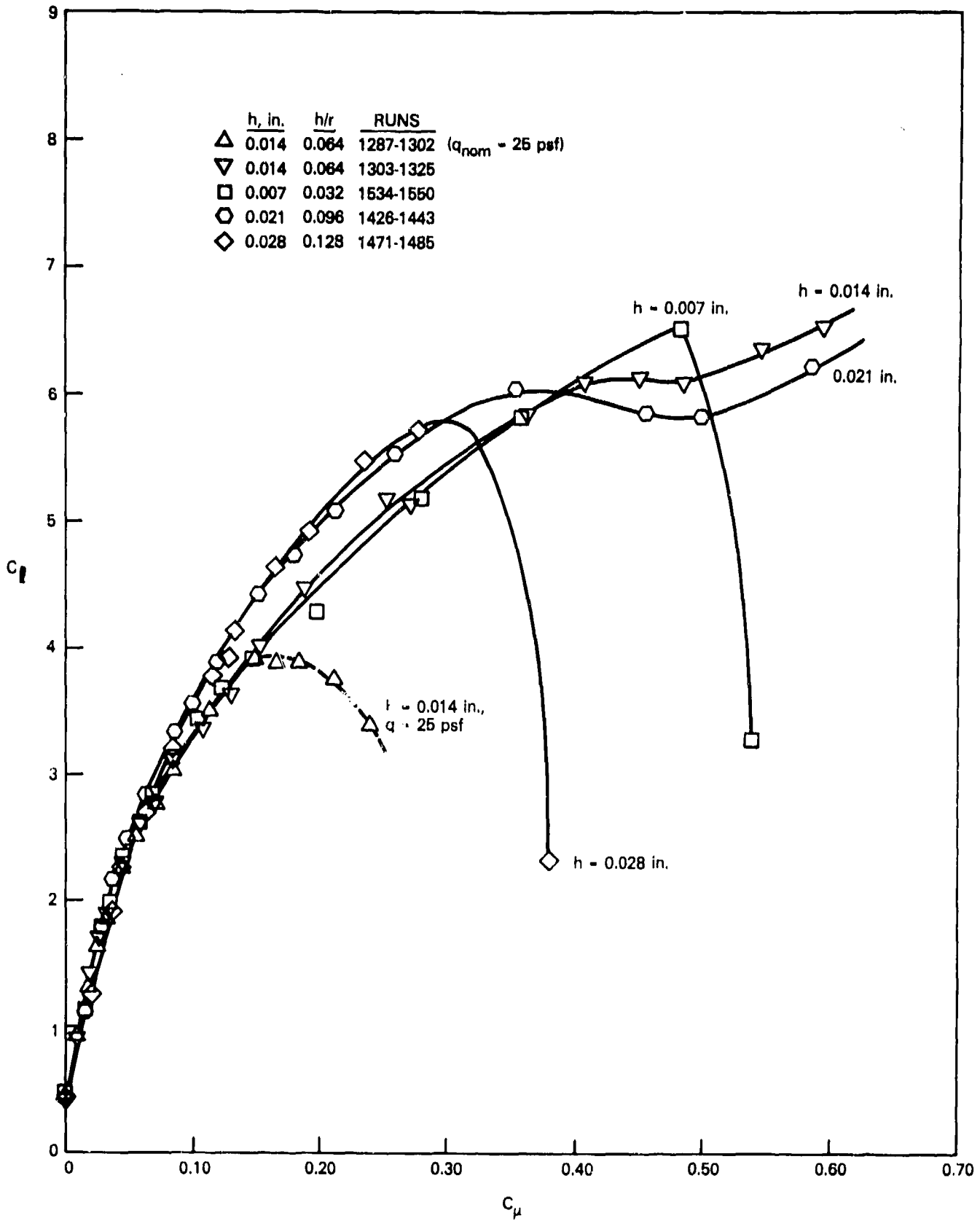


Figure 6d - Configuration 5, $r = 0.219$ Inches, $r/c' = 0.0094$

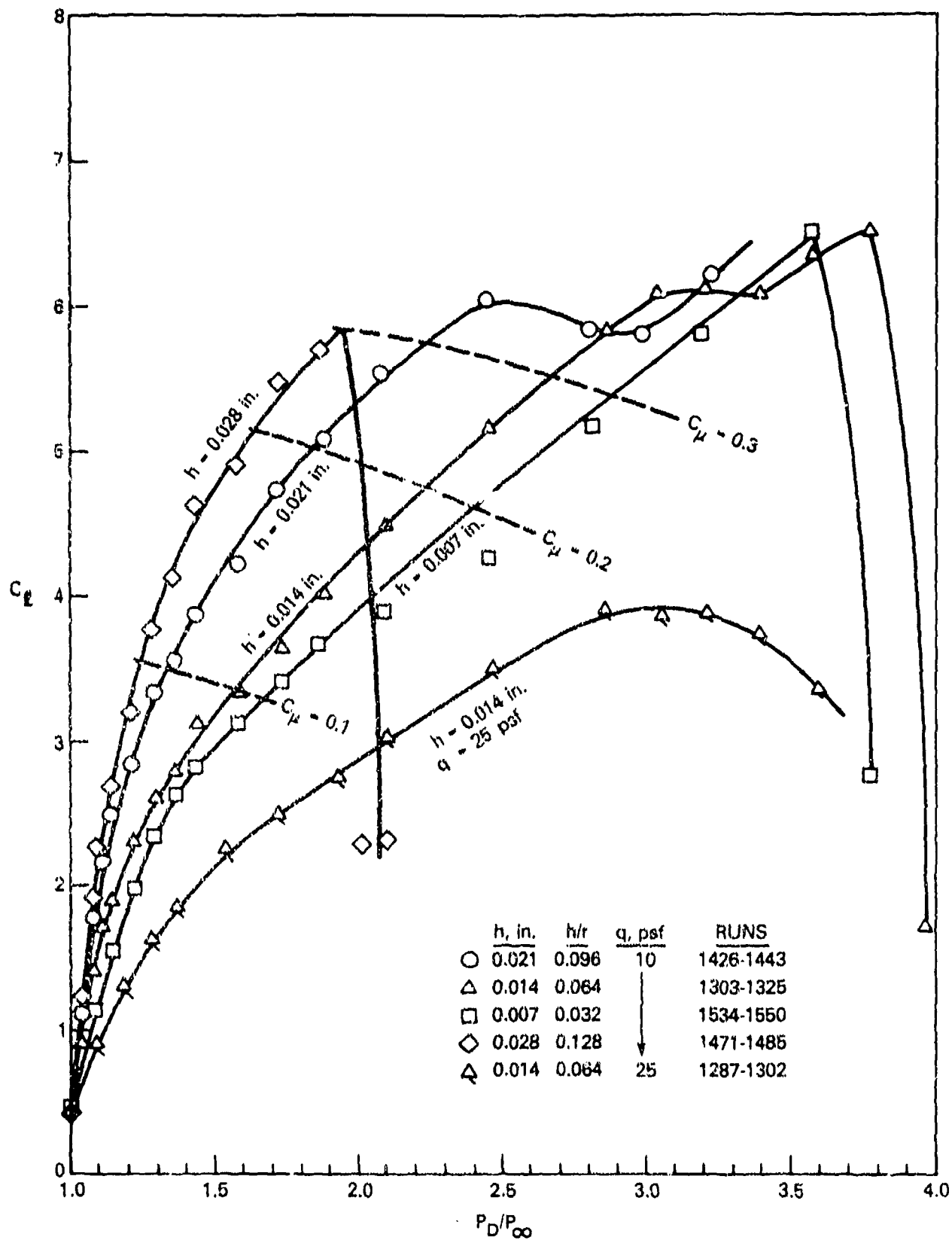


Figure 7 - Lift as a Function of Blowing Pressure Ratio for Configuration 5, $r = 0.219$ Inches

Figure 8 - Effect of Incidence Variation on Lift for Configuration 5, $r = 0.219$ Inches

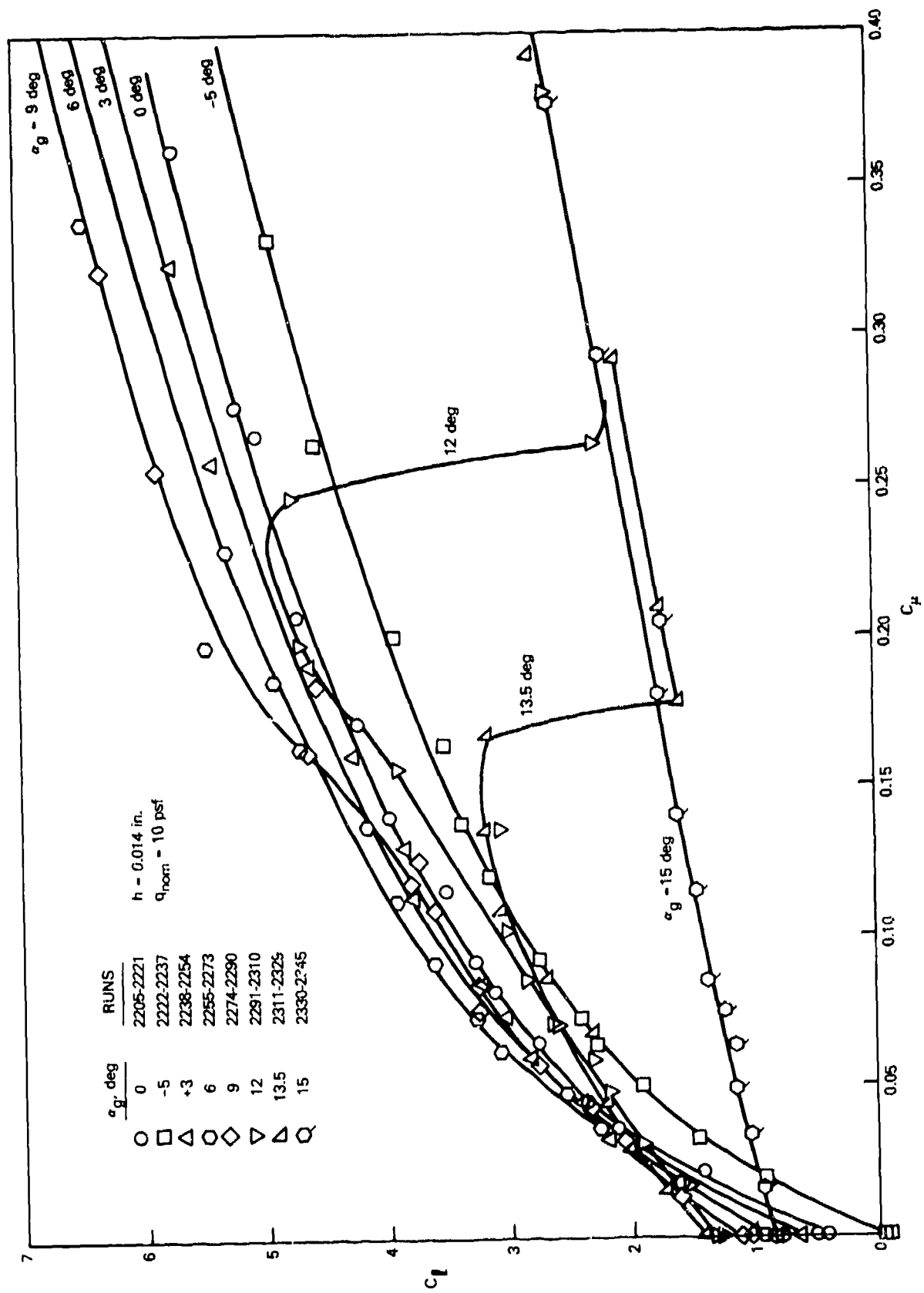


Figure 8a - Variation in Blowing at Constant Incidence

Figure 8 (Continued)

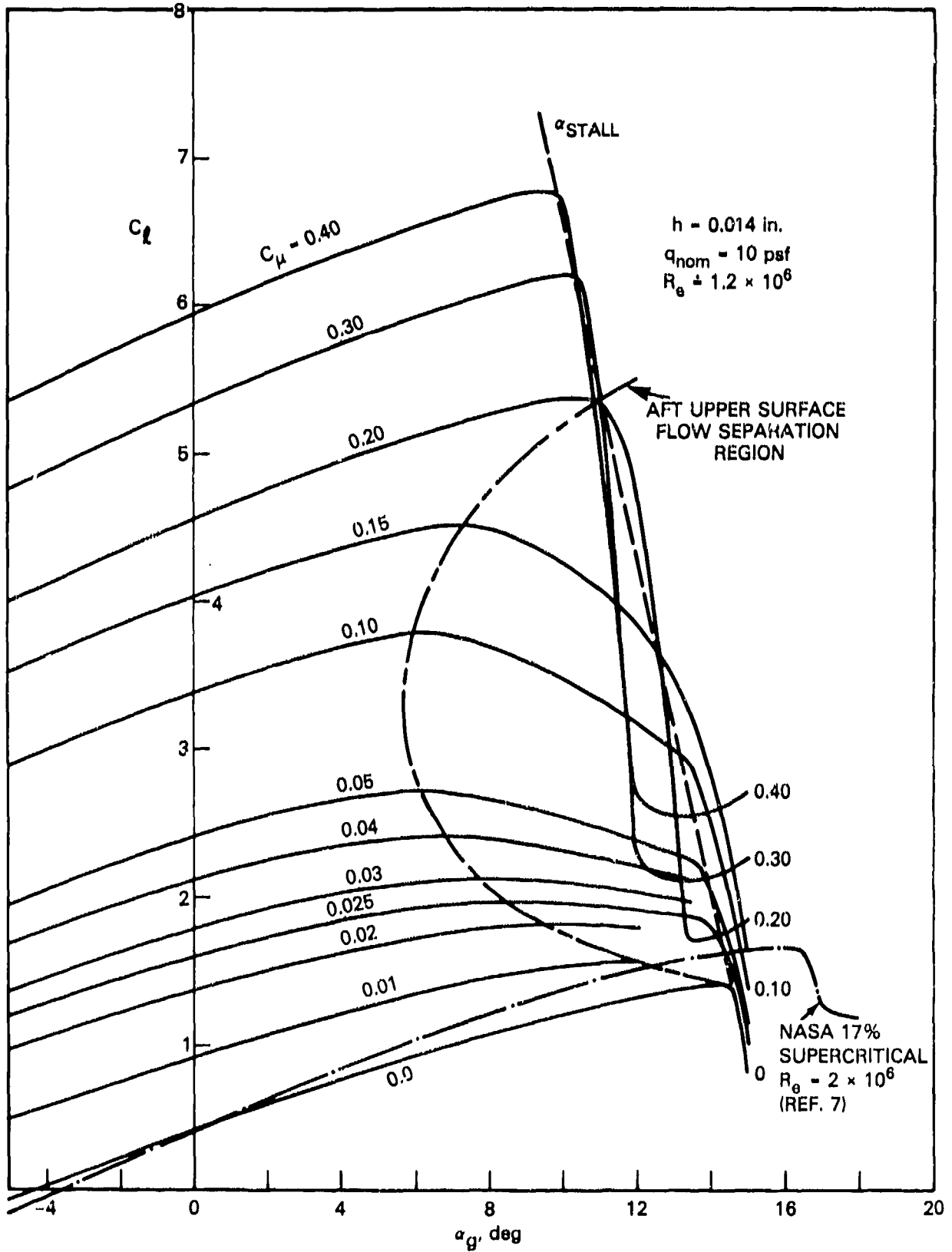


Figure 8b - Variation in Incidence at Constant Blowing

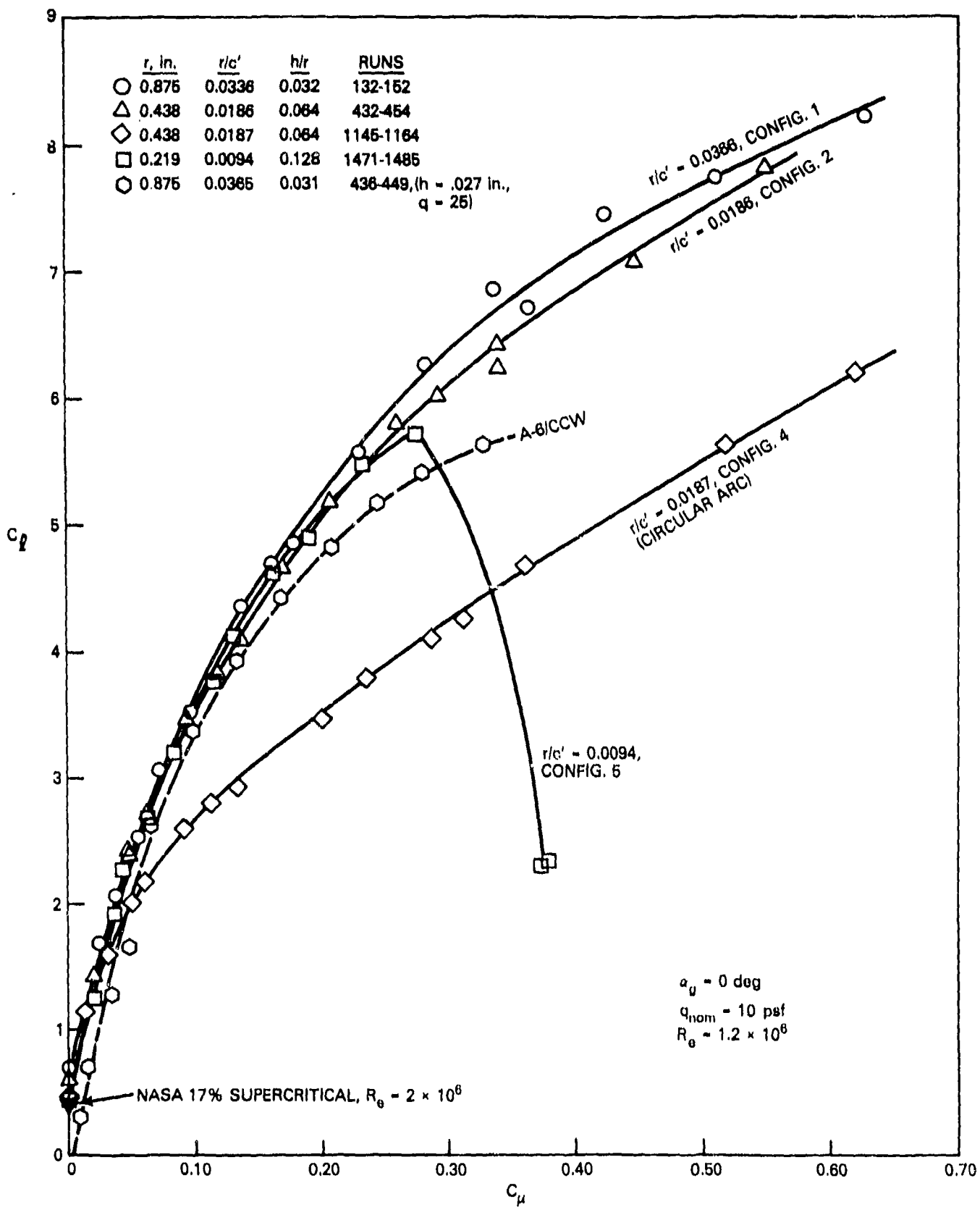


Figure 9 - Comparative CCW Airfoil Lift Performance, $h = 0.028$ Inches

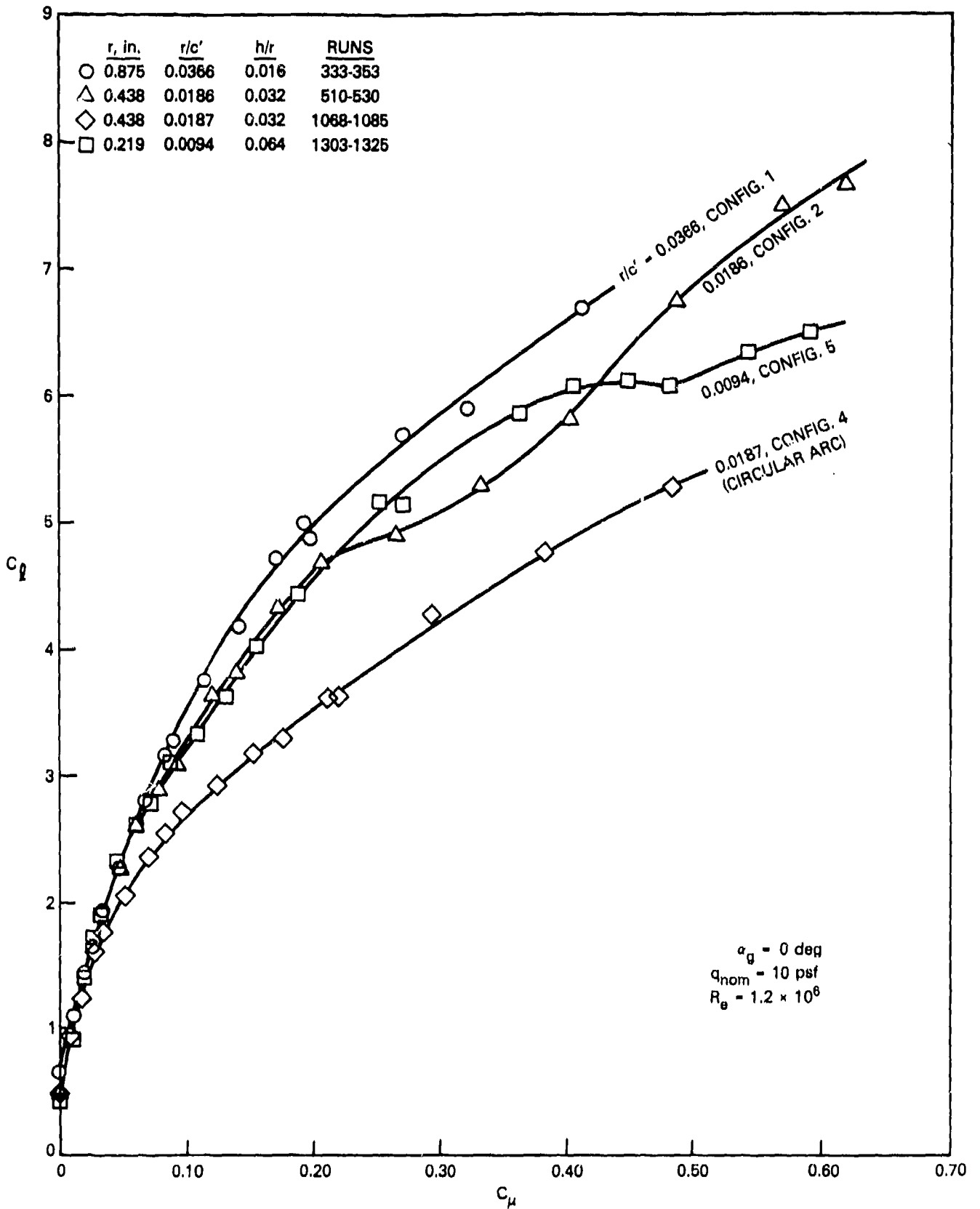


Figure 10 - Comparative CCW Airfoil Lift Performance, $h = 0.014$ Inches

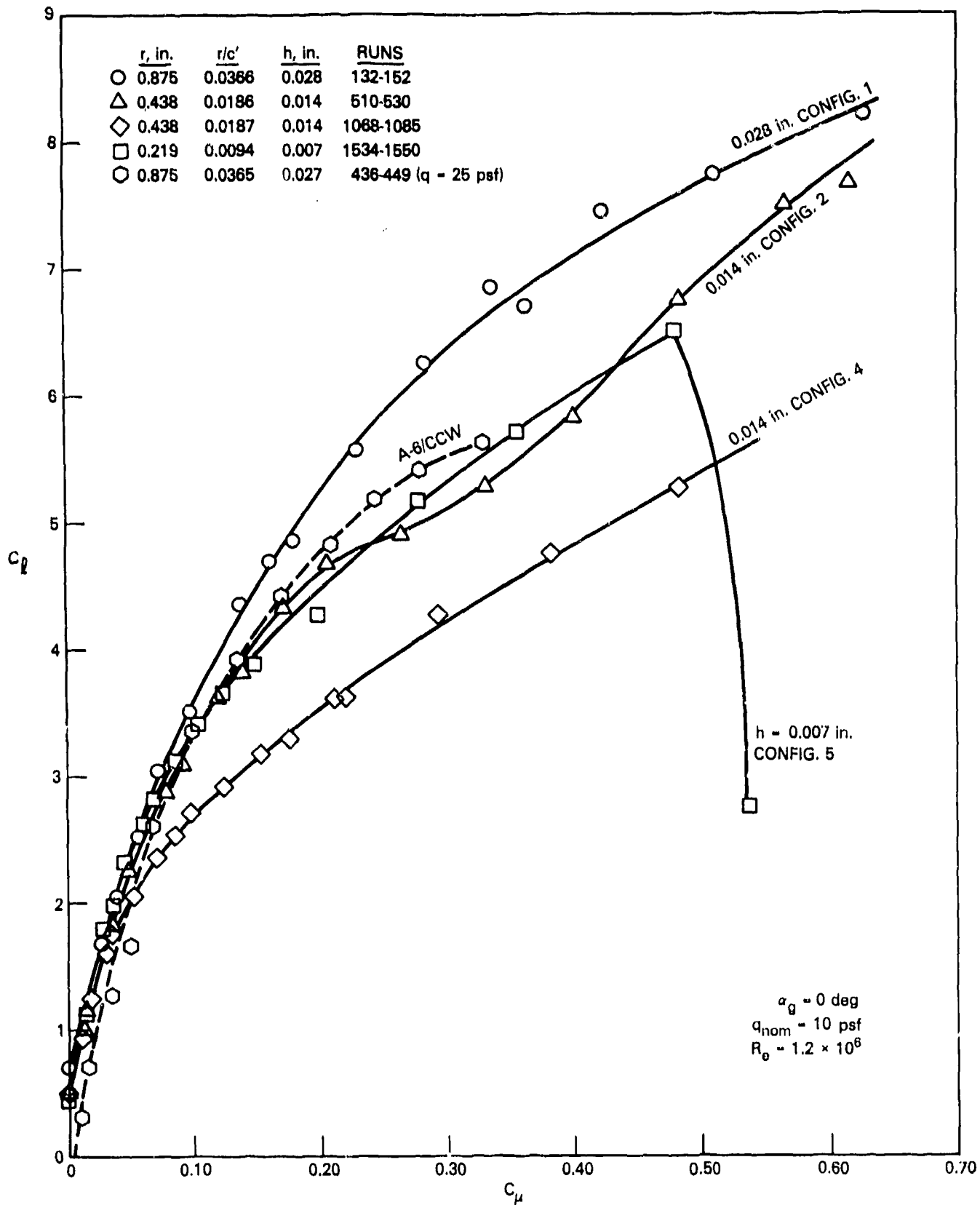


Figure 11 - Comparative CCW Airfoil Lift Performance, $h/r = 0.032$

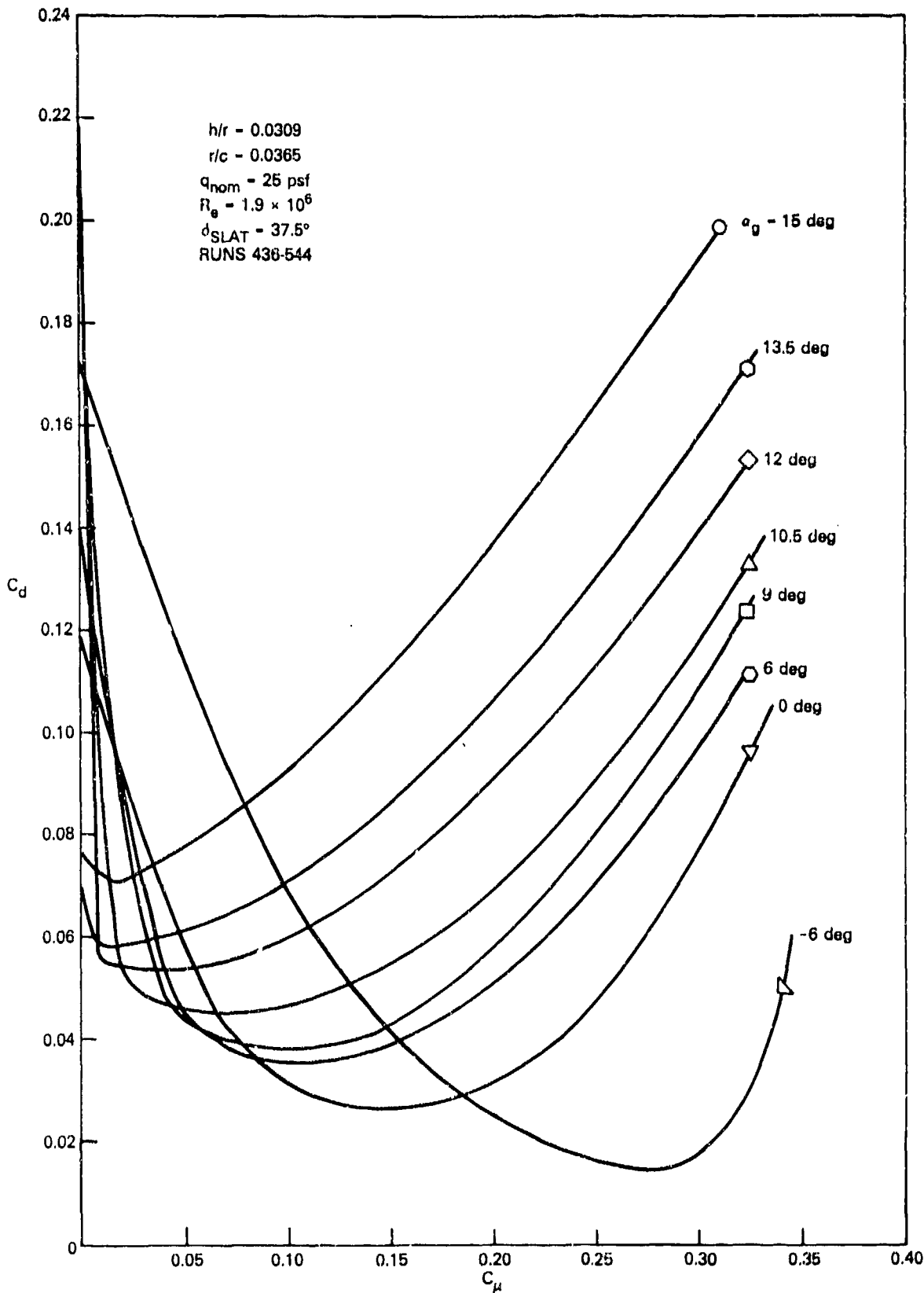


Figure 12 - Drag Characteristics of the NACA 64A008.4/CCW Airfoil (A-6/CCW Wing-Fold Section)

Figure 13 - Drag as a Function of Blowing and Slot Height for the CCW/Supercritical Airfoils at $\alpha_g = 0$ Degrees and $q_{nom} = 10$ PSF

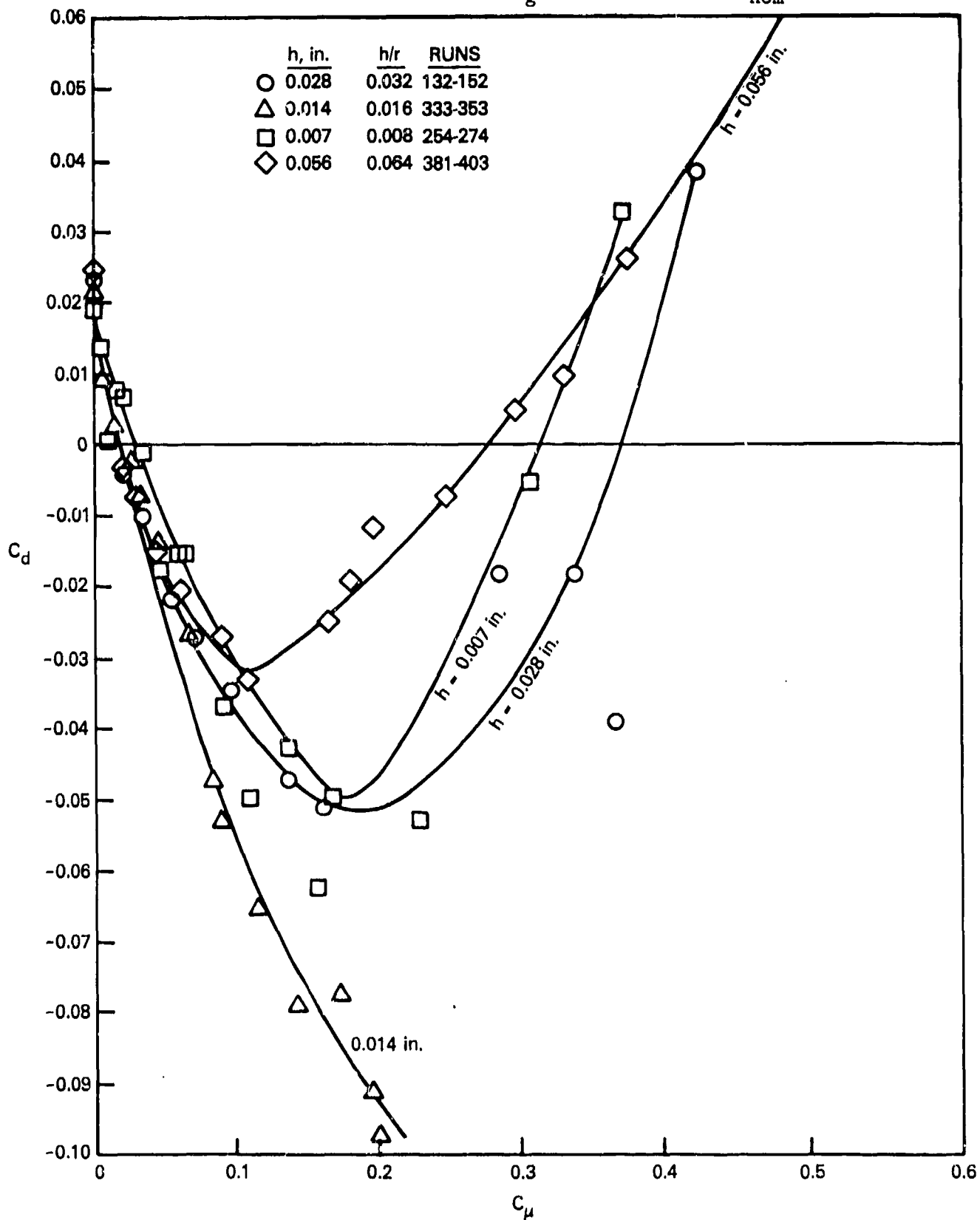


Figure 13a - Configuration 1, $r = 0.875$ Inches, $r/c' = 0.0366$

Figure 13 (Continued)

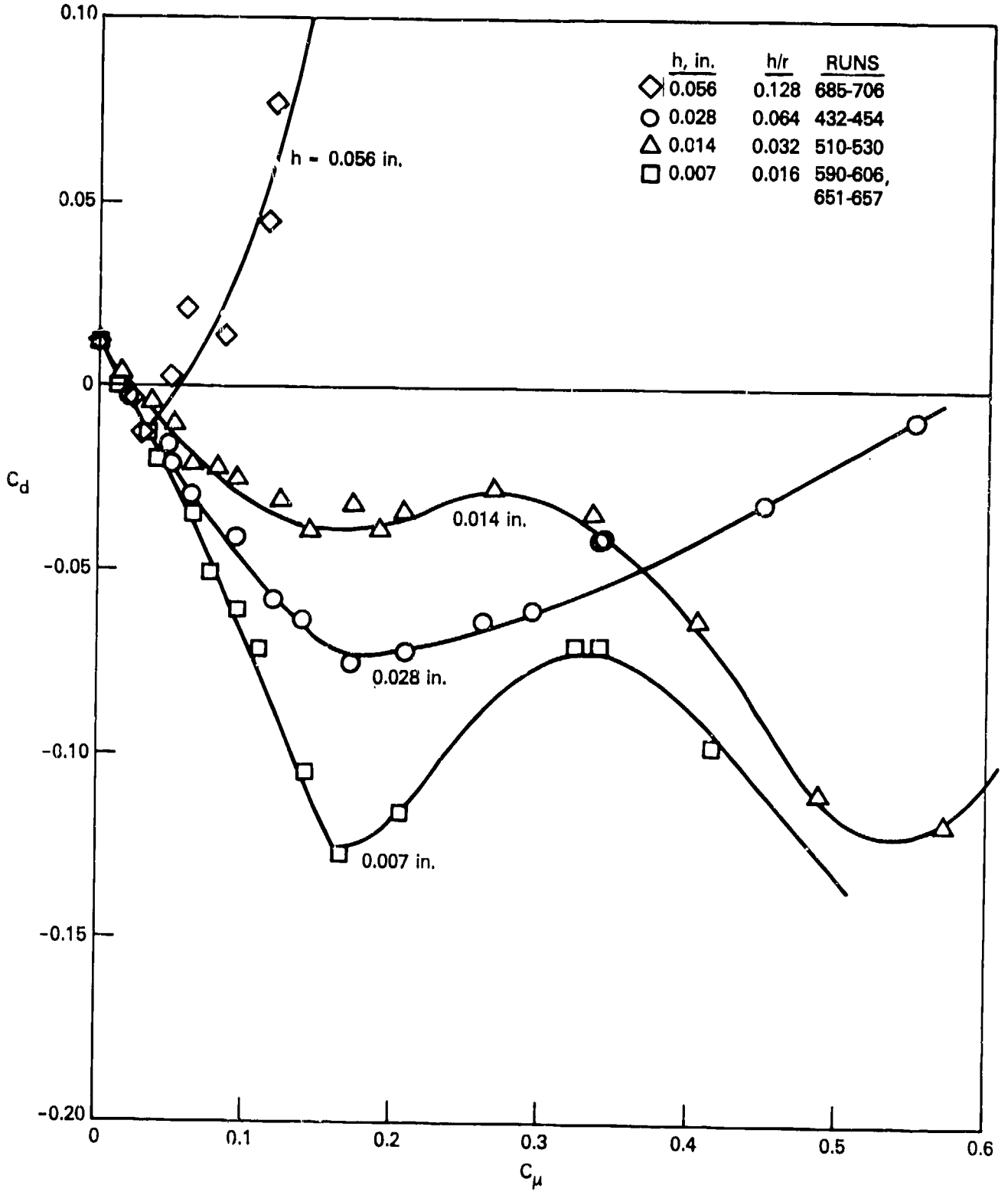


Figure 13b -- Configuration 2, $r = 0.438$ Inches, $r/c' = 0.0186$

Figure 13 (Continued)

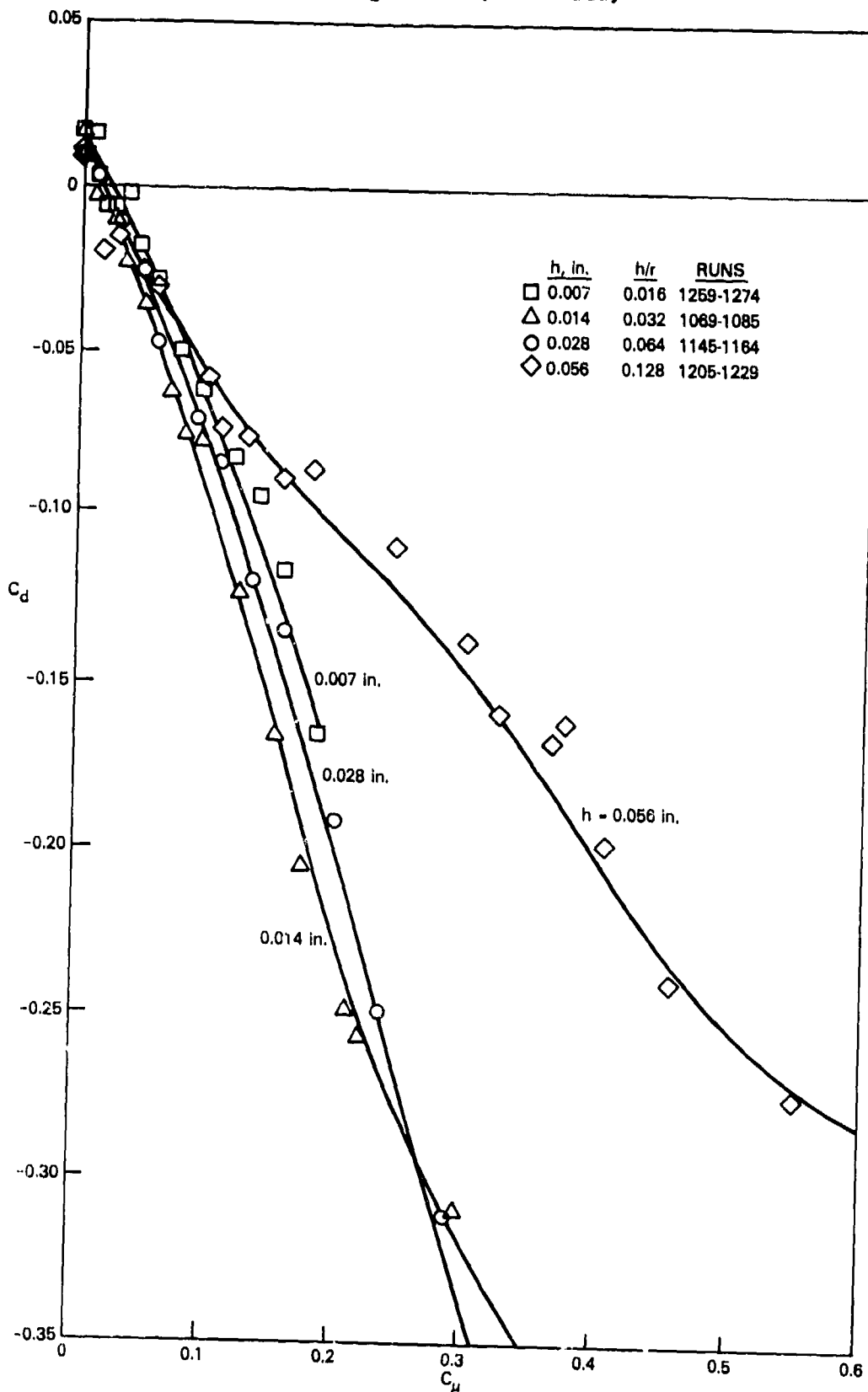


Figure 13c - Configuration 4, 96-Degree Circular Arc,
 $r = 0.438$ Inches, $r/c' = 0.0187$

Figure 13 (Continued)

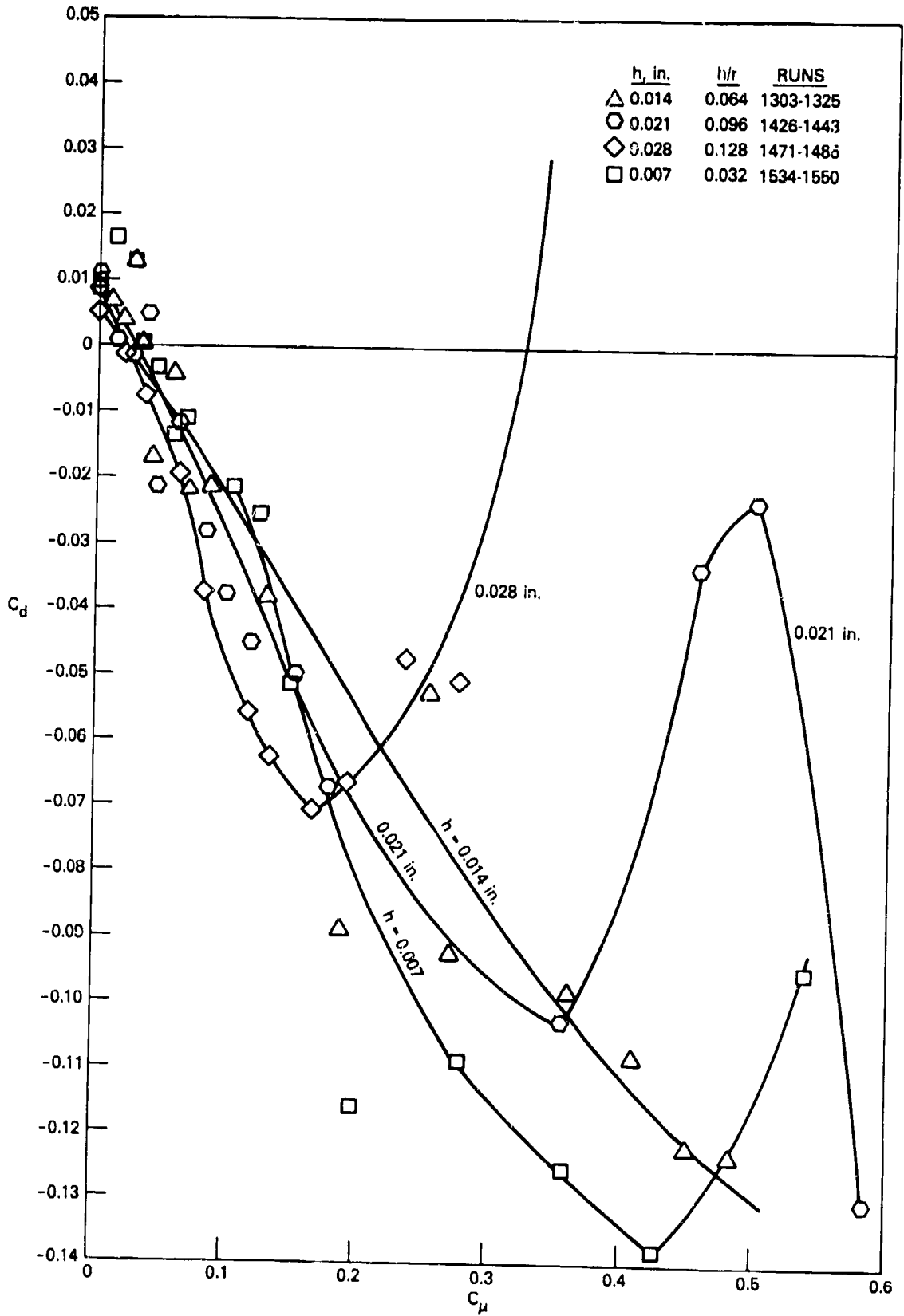


Figure 13d - Configuration 5, $r = 0.219$ Inches, $r/c' = 0.0094$

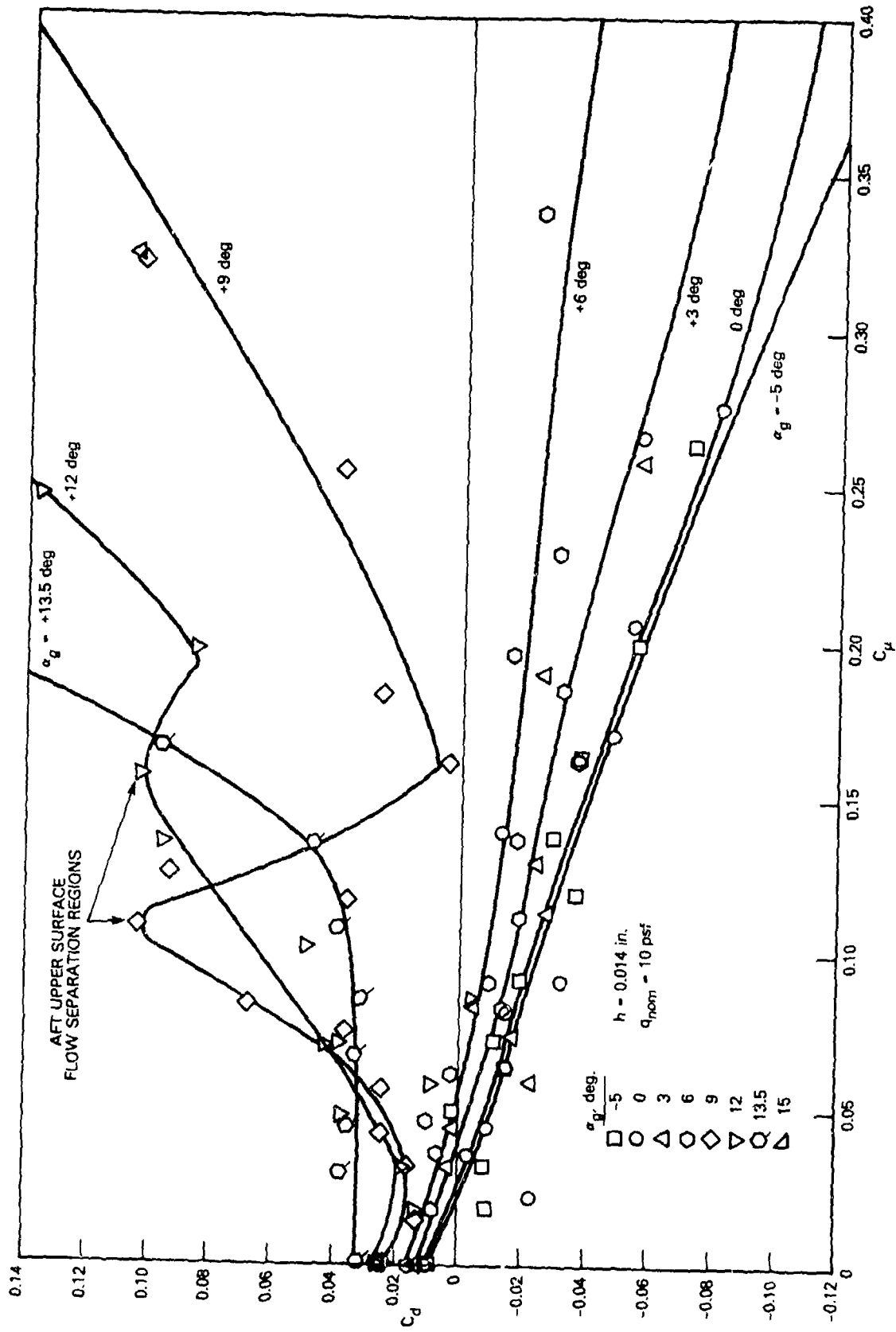


Figure 14 - Drag as a Function of Blowing and Incidence for Configuration 5, $r = 0.219$ Inches

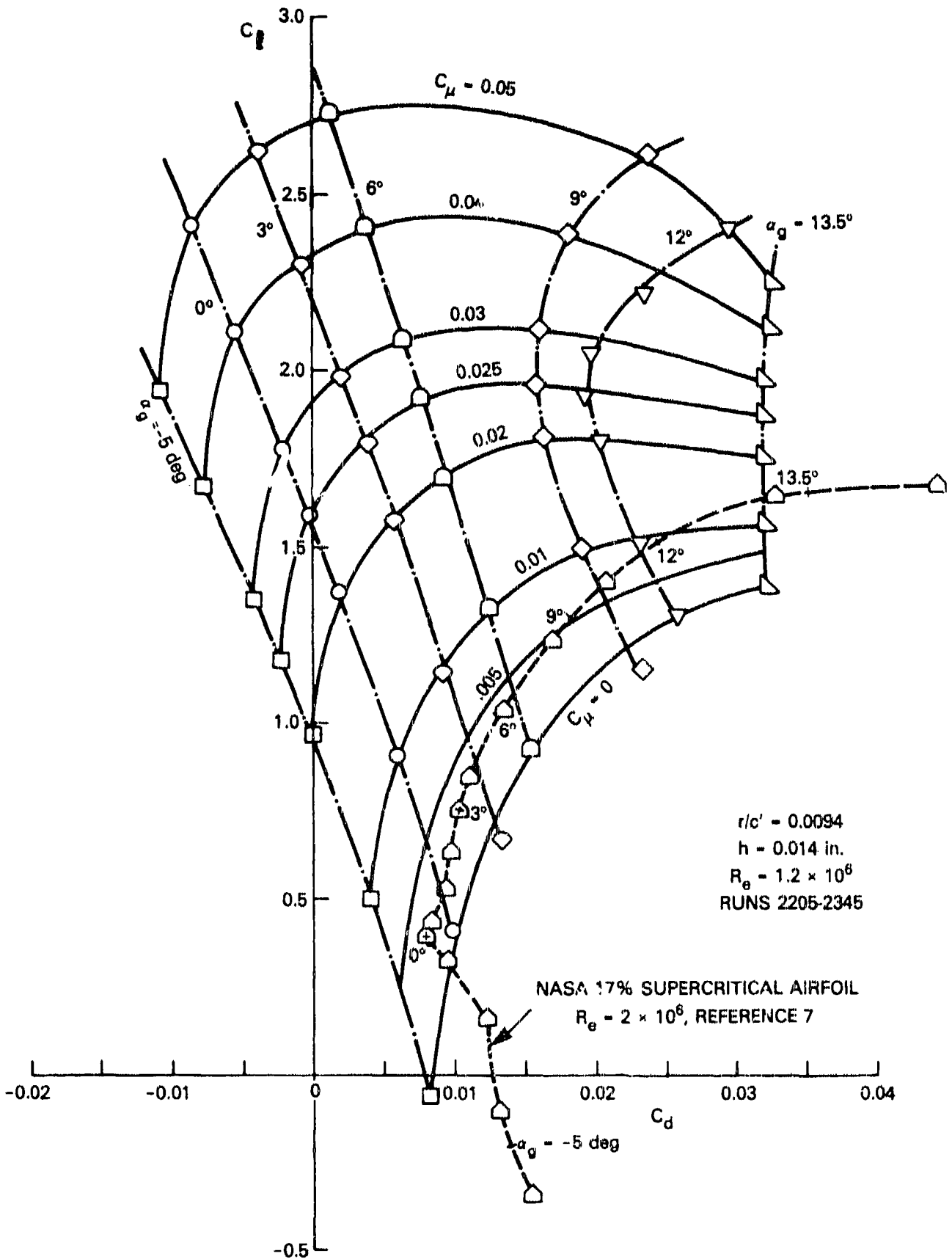


Figure 15 - Drag Polars for CCW/Supercritical Configuration 5 (r = 0.219 Inches) at Low Blowing

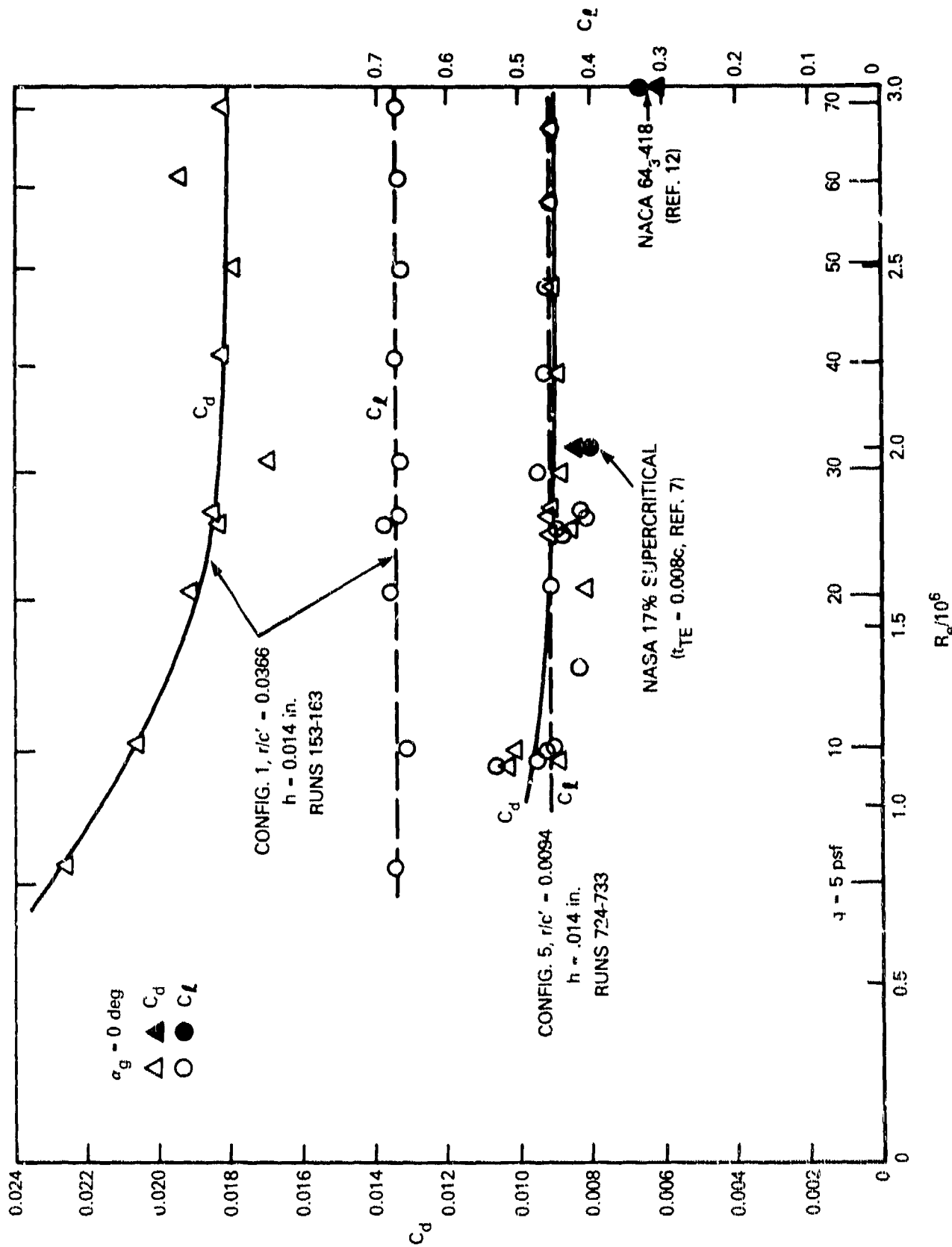


Figure 16 - Unblown Lift and Drag Comparisons as Functions of Reynolds Number at $\alpha_g = 0$ Degrees

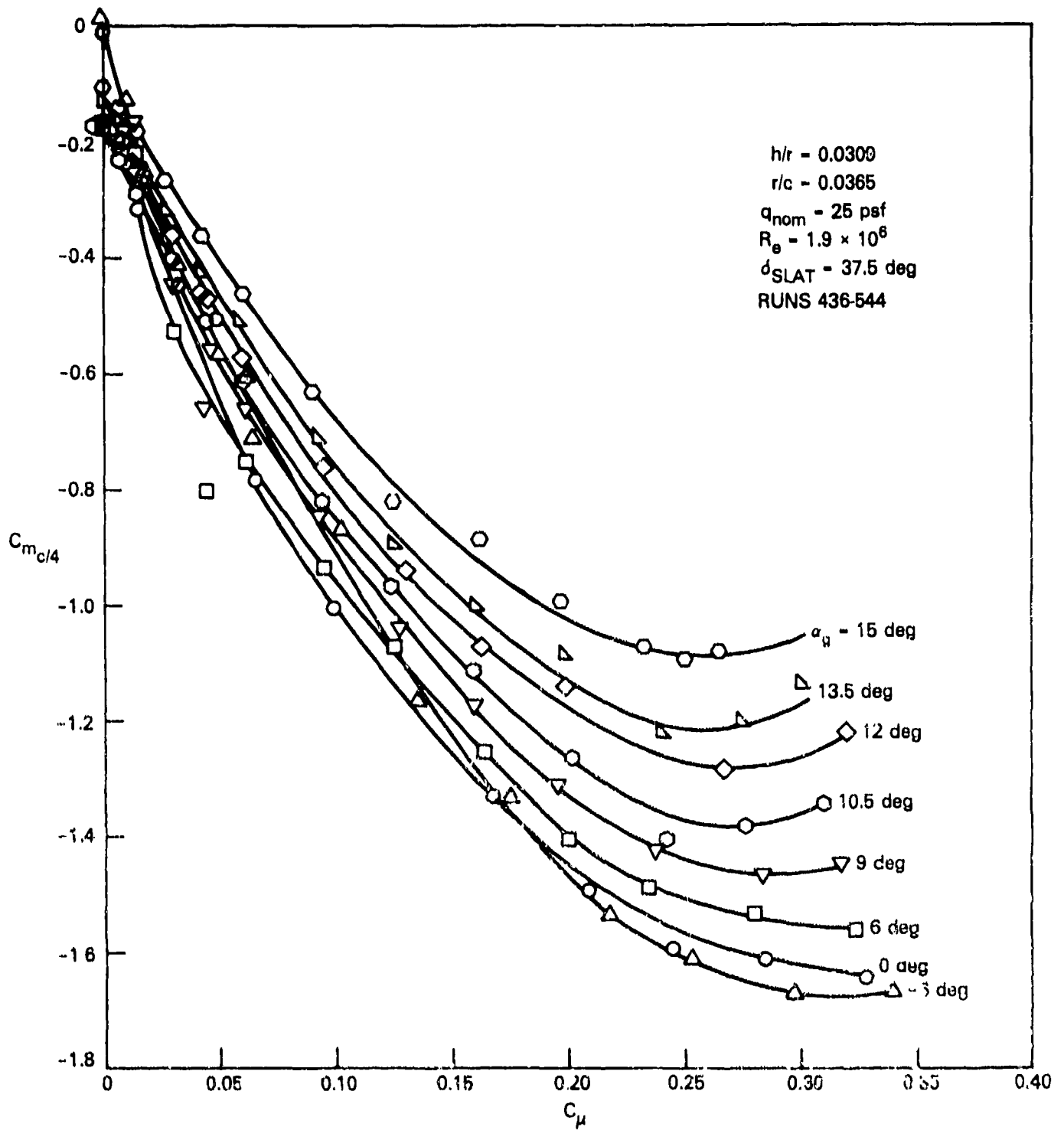


Figure 17 - Pitching-Moment Characteristics of the NACA 64A008.4/CCW Airfoil (A-6/CCW Wing-Fold Section)

Figure 18 - Pitching Moment as a Function of Blowing and Slot Height for the CCW/Supercritical Airfoils at $\alpha_g = 0$ Degrees and $q_{nom} = 10$ PSF

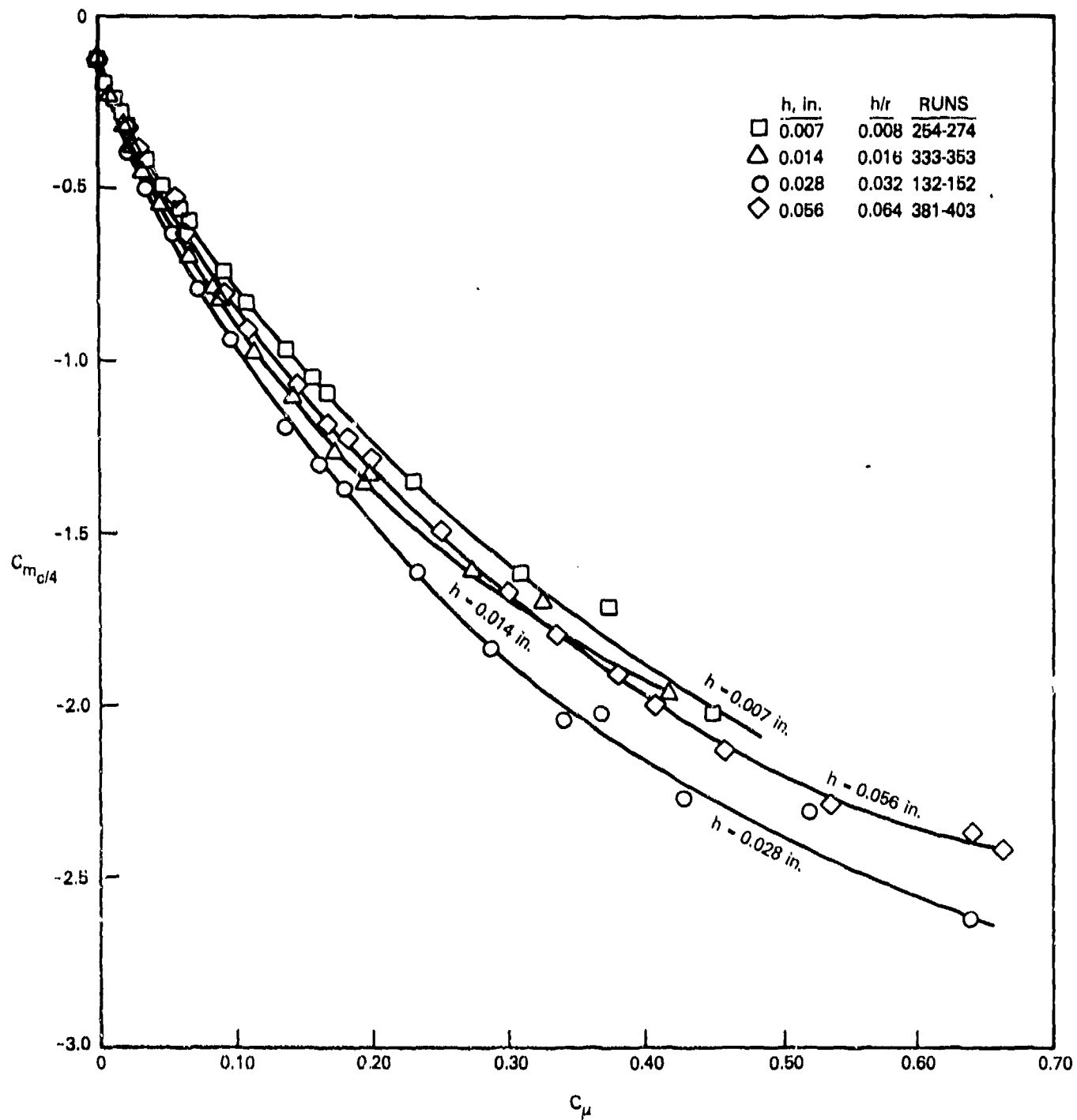


Figure 18a - Configuration 1, $r = 0.875$ Inches, $r/c' = 0.0366$

Figure 18 (Continued)

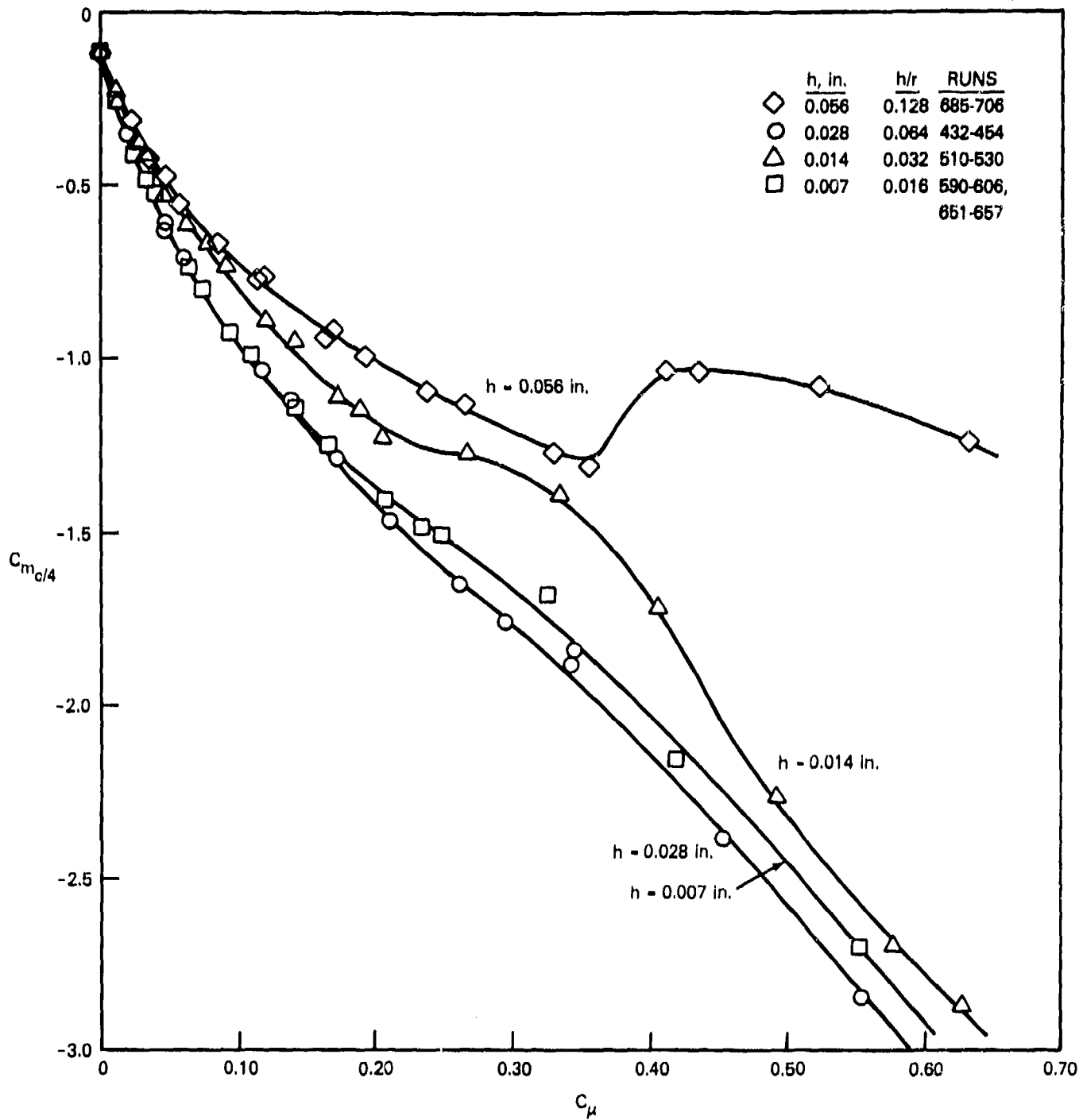


Figure 18b - Configuration 2, $r = 0.438$ Inches, $r/c' = 0.0186$

Figure 18 (Continued)

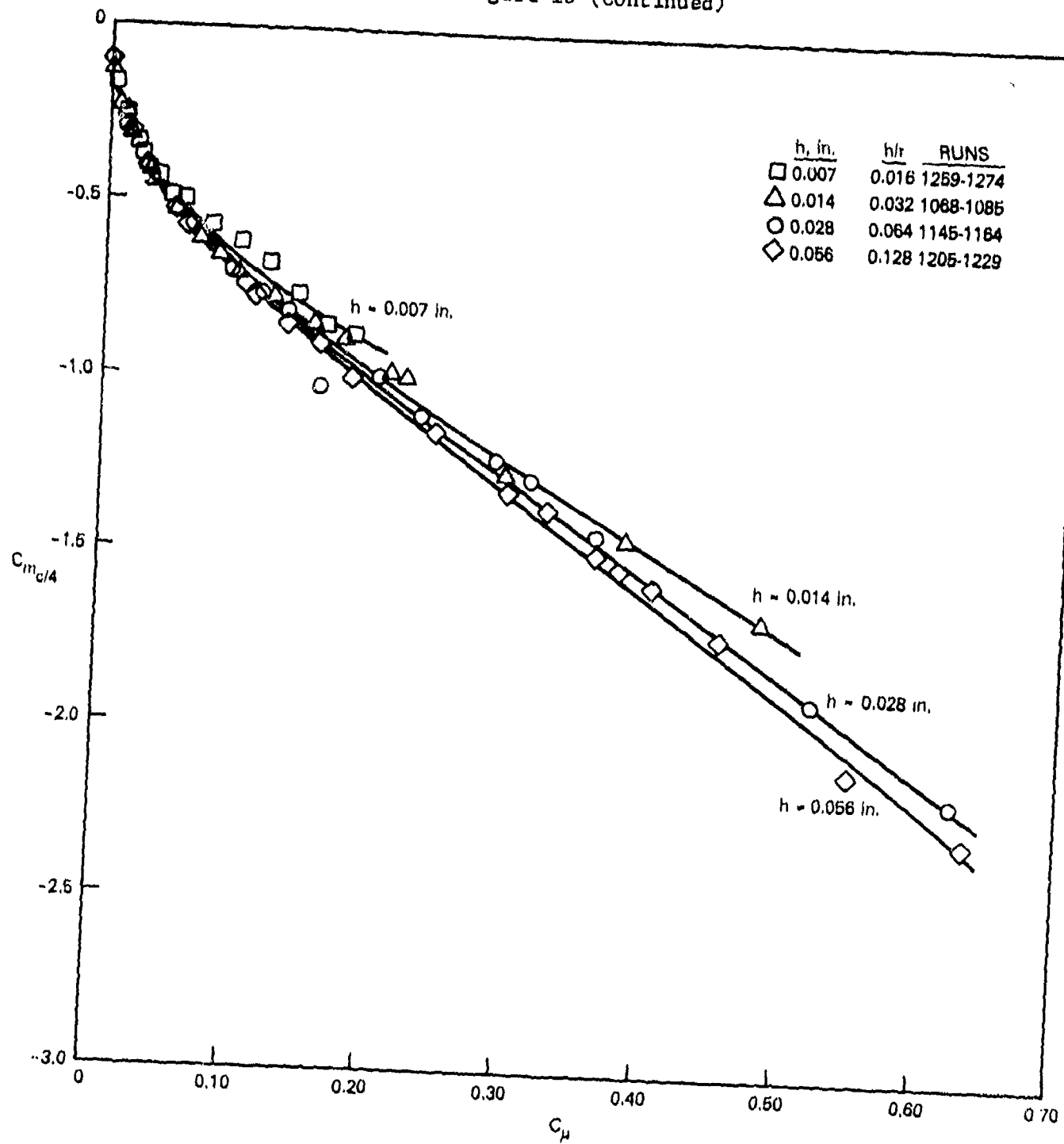


Figure 18c - Configuration 4, 96-Degree Circular Arc,
 $r = 0.438$ Inches, $r/c' = 0.0187$

Figure 18 (Continued)

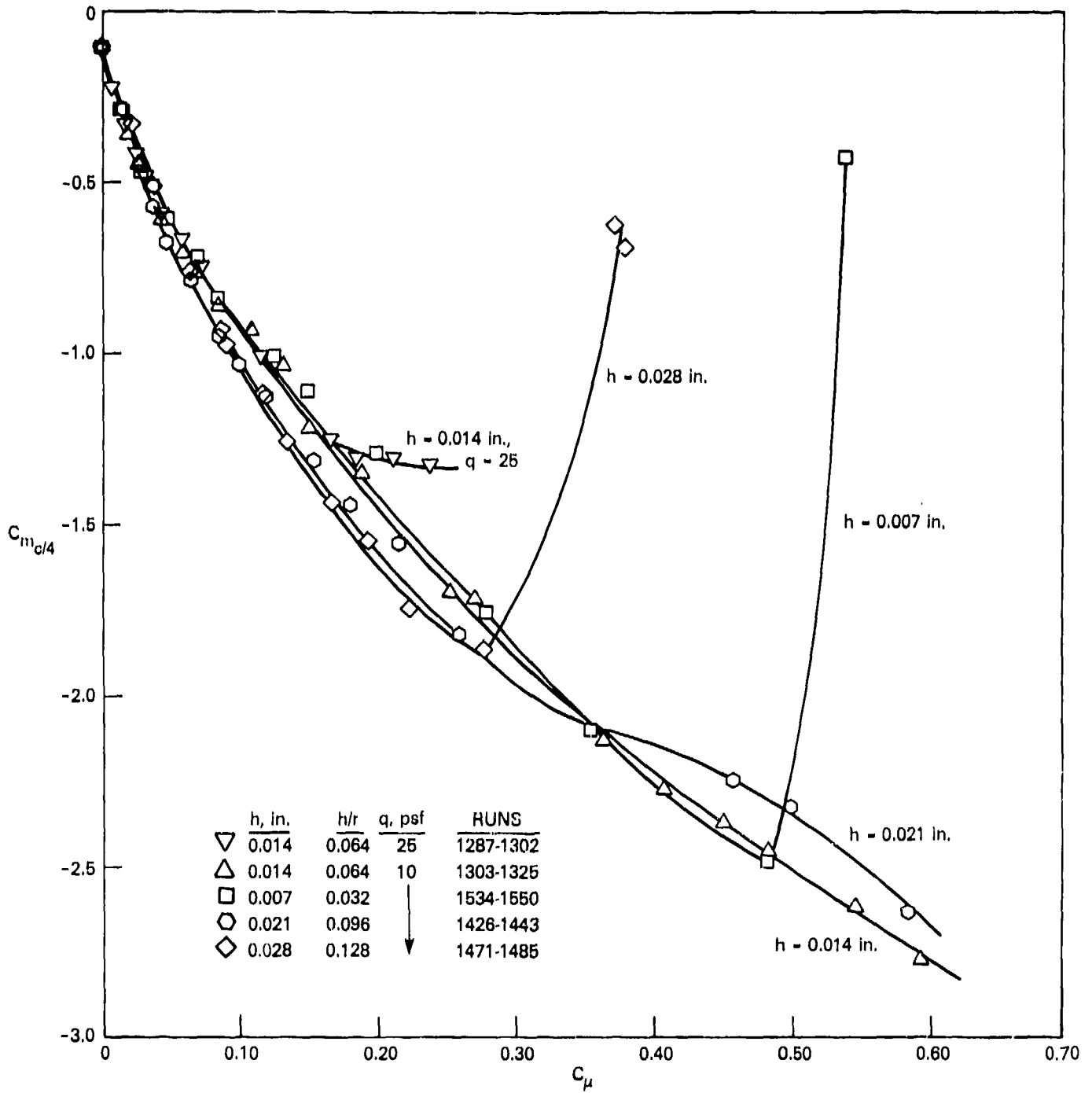


Figure 18d - Configuration 5, $r = 0.219$ Inches, $r/c' = 0.0094$

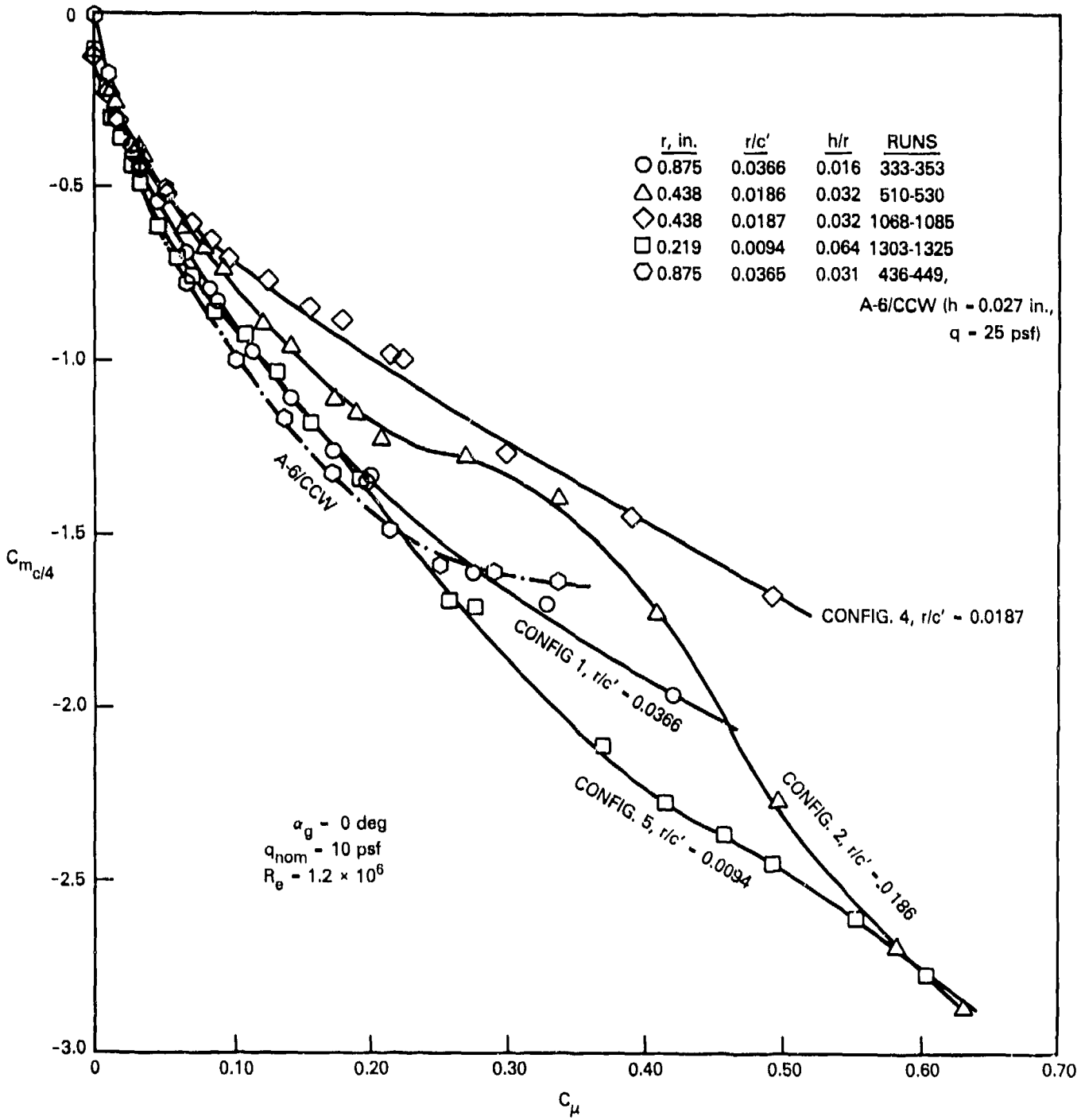


Figure 19 - Comparative CCW Airfoil Pitching Moment, $h = 0.014$ Inches

DTNSHDC ISSUES THREE TYPES OF REPORTS

- 1. DTNSRDC REPORTS, A FORMAL SERIES, CONTAIN INFORMATION OF PERMANENT TECHNICAL VALUE. THEY CARRY A CONSECUTIVE NUMERICAL IDENTIFICATION REGARDLESS OF THEIR CLASSIFICATION OR THE ORIGINATING DEPARTMENT.**
- 2. DEPARTMENTAL REPORTS, A SEMIFORMAL SERIES, CONTAIN INFORMATION OF A PRELIMINARY, TEMPORARY, OR PROPRIETARY NATURE OR OF LIMITED INTEREST OR SIGNIFICANCE. THEY CARRY A DEPARTMENTAL ALPHANUMERICAL IDENTIFICATION.**
- 3. TECHNICAL MEMORANDA, AN INFORMAL SERIES, CONTAIN TECHNICAL DOCUMENTATION OF LIMITED USE AND INTEREST. THEY ARE PRIMARILY WORKING PAPERS INTENDED FOR INTERNAL USE. THEY CARRY AN IDENTIFYING NUMBER WHICH INDICATES THEIR TYPE AND THE NUMERICAL CODE OF THE ORIGINATING DEPARTMENT. ANY DISTRIBUTION OUTSIDE DTNSRDC MUST BE APPROVED BY THE HEAD OF THE ORIGINATING DEPARTMENT ON A CASE-BY-CASE BASIS.**